Research Article

The *In Vitro* Human Fracture Hematoma Model – A Tool for Preclinical Drug Testing

Moritz Pfeiffenberger[1,2], Paula Hoff[1,3], Christa Thöne-Reineke[4], Frank Buttgereit[1,2], Annemarie Lang[1,2] and Timo Gaber[1,2]

[1]Charité – Universitätsmedizin Berlin, corporate member of Freie Universität Berlin, Humboldt-Universität zu Berlin, and Berlin Institute of Health, Department of Rheumatology and Clinical Immunology, Berlin, Germany; [2]German Rheumatism Research Centre (DRFZ) Berlin, a Leibniz Institute, Berlin, Germany; [3]Endokrinologikum Berlin am Gendarmenmarkt, Berlin, Germany; [4]Institute of Animal Welfare, Animal Behavior and Laboratory Animal Science, Department of Veterinary Medicine, Freie Universität Berlin, Berlin, Germany

Abstract

The aim of the study was to establish an *in vitro* fracture hematoma (FH) model that mimics the *in vivo* situation of the human fracture gap in order to assess drug efficacy and effectiveness for the treatment of fracture healing disorders. Human peripheral blood and mesenchymal stromal cells (MSCs) were coagulated to produce *in vitro* FH models, which were incubated in osteogenic medium under normoxia/hypoxia and analyzed for cell composition, gene expression and cytokine/chemokine secretion. To evaluate the model, we studied the impact of dexamethasone (impairing fracture healing) and deferoxamine (promoting fracture healing). Under hypoxic conditions, MSCs represented the predominant cell population, while the frequencies of leukocyte populations decreased. Marker gene expression of osteogenesis, angiogenesis, inflammation, migration and hypoxic adaptation increased significantly over time and compared to normoxia, while cytokine/chemokine secretion remained unchanged. Dexamethasone favored the frequency of immune cells compared to MSCs, suppressed osteogenic and pro-angiogenic gene expression, and enhanced the secretion of inflammatory cytokines. Conversely, deferoxamine favored the frequency of MSCs over that of immune cells and enhanced the expression of the osteogenic marker *RUNX2* and markers of hypoxic adaptation. In summary, we demonstrate that hypoxia is an important factor for modeling the initial phase of fracture healing *in vitro* and that both fracture-healing disrupting and promoting substances can influence the *in vitro* model comparable to the *in vivo* situation. Therefore, we conclude that our model is able to mimic in part the human FH and could reduce the number of animal experiments in early preclinical studies.

1 Introduction

The healing of approximately 10% of bone fractures is impaired, and this is accompanied by pain and suffering of the affected patients and tremendous socio-economic costs (Gomez-Barrena et al., 2015; Gaston and Simpson, 2007). During the process of fracturing, the bone marrow canal is opened and adjacent blood vessels rupture. The cells emerging from the bone marrow (e.g., mesenchymal stromal cells – MSCs, hematopoietic progenitor cells and premature lymphocytes) mix with peripheral blood in the fracture gap, coagulate and form the fracture hematoma (FH). Local inflammation appears to promote the migration and recruitment of MSCs, endothelial cells, immune cells and fibroblasts (Kolar et al., 2010). Particularly MSCs are considered to play a pivotal role in an adequate healing process, since they are able to differentiate into both chondrocytes and osteoblasts/osteocytes, thereby facilitating bone healing (Knight and Hankenson, 2013). The transcription factor runt-related transcription factor (RUNX2) drives MSCs towards the osteogenic lineage, while its secreted downstream target phosphoprotein 1 (SPP1) is a key marker for early osteogenesis and is also induced by hypoxia-inducible factor 1 (HIF-1; HIF1A) (Gross et al., 2005; Li et al., 2004). Furthermore, matrix metalloproteinase 2 (MMP2) and MMP9, which are fundamental for appropriate bone healing (Henle et al., 2005), are induced via the HIF-1 pathway (Luo et al., 2006; O'Toole et al., 2008).

Received October 21, 2019; Accepted May 28, 2020;
Epub June 9, 2020; © The Authors, 2020.

ALTEX 37(4), 561-578. doi:10.14573/altex.1910211

Correspondence: Timo Gaber, PhD
Charité – Universitätsmedizin Berlin
corporate member of Freie Universität Berlin
Humboldt-Universität zu Berlin, and Berlin Institute of Health
Department of Rheumatology and Clinical Immunology
Charitéplatz 1, 10117 Berlin, Germany
(timo.gaber@charite.de)

Additionally, MSCs can attract other cells that are crucial for the ongoing regeneration process such as T cells, granulocytes and macrophages towards the fracture site. In brief, MSCs in a pro-inflammatory microenvironment distinctly secrete chemokine (C-X-C motif) ligand (CXCL)9, CXCL10, macrophage inflammatory protein (MIP)-1α, MIP-1β and Rantes, thereby enhancing lymphocyte recruitment. Additionally, granulocytes are recruited through the enhanced secretion of granulocyte-macrophage colony-stimulating factor (GM-CSF), interleukin 6 (IL-6) and IL-8 (Le Blanc and Davies, 2015).

During the initial phase of fracture healing, i.e., within the first 1-5 days after the fracture (Annamalai et al., 2018), immune cells play a pivotal role. Their inflammatory activity can be considered a double-edged sword for the bone healing process. Although useful in initiating the bone healing process by recruiting MSCs and endothelial cells to the fracture site via cytokine signaling, immune cells also prolong the healing process by perpetuating the inflammatory response (El-Jawhari et al., 2016). More in detail, granulocytes as well as monocytes/macrophages and natural killer (NK) cells are involved in the clearance of debris (Baht et al., 2018; Thomas and Puleo, 2011), NK-cells recruit MSCs towards the fracture site, while monocytes/macrophages conduct re-vascularization. T cells are assumed to orchestrate the inflammatory process during the initial phase of fracture healing by retaining but also attenuating the inflammation (El-Jawhari et al., 2016). However, the distinct roles of immune cell populations and their temporal and spatial distribution and composition within the FH still remain unclear.

Due to the disruption of the blood supply, the FH is characterized by a severe lack of nutrients and oxygen (Hoff et al., 2016). Cellular adaptation towards the hypoxic microenvironment of the fracture gap is mainly driven by HIF-1, which regulates the switch from oxidative phosphorylation towards glycolysis and also promotes the reestablishment of vascularization (Cramer et al., 2003). HIF-1 induces genes of the glycolytic cascade such as phosphoglycerate kinase (PGK1) and lactate dehydrogenase (LDHA), and genes encoding pro-angiogenic factors such as vascular endothelial growth factor (VEGFA) and IL-8 (Liu et al., 2012; Dengler et al., 2014). The inflammatory milieu in the FH is *inter alia* characterized by the presence of pro-inflammatory cytokines, e.g., IL-6 and IL-8, which are abundantly secreted during the initial phase leading to cell activation, and the recruitment of further immune cells into the fracture site via, e.g., CXC-motif chemokine receptor 4 (CXCR4) (Liu et al., 2012). Especially the initial phase of fracture healing within the FH is susceptible to fracture healing disorders, which can lead to delayed or even incomplete healing of the affected bone (Claes et al., 2012; Schindeler et al., 2008).

The experimental removal of the FH in a rat femoral fracture model prolonged the healing process (Grundnes and Reikeras, 1993), while the implantation of a FH improved bone healing (Mizuno et al., 1990; Tachibana et al., 1991). Specifically, Mizuno et al. (1990) transplanted the hematoma of the rat's femur to subperiosteal sites, observing new bone formation there, indicating strong osteogenic potential. Tachibana et al. (1991) used fluid material of human FHs, which induced osteoblast proliferation in the osteoblast-like cell line MC3T3E1.

Until now, research concerning fracture healing is most often performed using animal, particularly rodent, models (mice and rats). Not only the size of the rodents differs from human patients (Perlman, 2016); also the similarity of the inflammatory process in rodents and men is controversially discussed (Mestas and Hughes, 2004; Seok et al., 2013; Takao and Miyakawa, 2015). Apart from the advantages of using mice to study certain pathways and systemic effects (e.g., easy to handle, requirement of little space, gene editing possible), the difference in species-specific evolutionary pressure and the resulting molecular and anatomical differences have to be considered carefully in evaluating the relevance of the rodent model. These differences include the lack of the Haversian system, a microtubule system that provides the space for blood vessels and nerves to grow (Bagi et al., 2011; Jowsey, 1966).

We previously studied the cell composition, RNA and cytokine profile of FHs obtained from human patients (Hoff et al., 2013, 2016; Kolar et al., 2010, 2011). Based on these findings, we here developed a human *in vitro* model of the FH in order (i) to mimic the initial phase of fracture healing, (ii) to contextualize the obtained data to existing *ex vivo* and *in vivo* data, and (iii) to use this system to analyze the impact of drugs/therapies relevant for fracture healing in order to (iv) reduce animal numbers in research and accelerate translation in this area.

2 Materials and methods

Blood sampling, bone marrow-derived MSC isolation and cultivation

Blood was collected in 6 mL EDTA Vacutainers (Becton Dickinson, Franklin Lakes, USA) from healthy donors.

Human mesenchymal stromal cells (hMSCs) were isolated from bone marrow of patients undergoing total hip replacement (provided by the Center for Musculoskeletal Surgery, Charité-Universitätsmedizin Berlin and distributed via the "Tissue Harvesting" core facility of the BCRT). All procedures were approved by the Charité-Universitätsmedizin Ethics Committee and were performed according to the Helsinki Declaration (ethical approval EA1/012/13).

Bone marrow was transferred to a 175 cm^2 cell tissue flask (Greiner Bio-one, Kremsmünster, Austria) and incubated in DMEM + GlutaMAX™ (Gibco, Carlsbad, USA) supplemented with 10% FCS (Biowest, Riverside, USA), 1% Penicillin/Streptomycin (Gibco, Carlsbad, USA) and 20% StemMACS™ MSC Expansion Media Kit XF (Miltenyi Biotech, Bergisch Gladbach, Germany) in a humidified atmosphere (37°C, 5% CO_2, 95% room air). After 2 days of cultivation, the supernatant was discarded, and the adherent cells were washed three times using PBS. From then on, the cell culture medium was changed once a week; cells with a confluence of 80-90% were passaged using Trypsin-EDTA. Bone marrow-derived non-differentiated hMSCs in passage 3-4 were used for all FH models.

In order to replace FCS during MSC propagation, we used xeno-free 20% StemMACS™ MSC Expansion Media Kit XF (Miltenyi Biotech, Bergisch Gladbach, Germany). When trying

Tab. 1: Blood donors and MSC donors for the generation of the *in vitro* fracture hematomas

Donor	Cell type	Age	Sex	FH model	Impact of hypoxia[a]	Impact of DFO/DEX[a]
B1	blood	44	m	MSC1, MSC2	FC, GE, CCS	-
B2	blood	23	m	MSC1, MSC2	FC, GE, CCS	-
B3	blood	27	m	MSC1, MSC2	FC, GE, CCS	-
MSC1	bmMSCs	77	m	B1, B2, B3	FC, GE, CCS	-
MSC2	bmMSCs	75	m	B1, B2, B3	FC, GE, CCS	-
B4	blood	37	m	MSC3, MSC4	-	FC, GE, CCS
B5	blood	26	m	MSC3, MSC4	-	FC, GE, CCS
B6	blood	38	m	MSC3, MSC4	-	FC, GE, CCS
MSC3	bmMSCs	72	m	B4, B5, B6	-	FC, GE, CCS
MSC4	bmMSCs	62	m	B4, B5, B6	-	FC, GE, CCS

[a] FC, flow cytometry analysis; GE, gene expression analysis; CCS, cytokine/chemokine secretion analysis

to fully replace FCS by using pooled human platelet lysate according to the protocol of Schallmoser and Strunk (2009), we observed detachment of MSCs from the plastic surface of incubation chambers and additionally the absence of the typical characterization marker CD90 as determined by flow cytometry. Thus, we had to postpone the replacement of FCS, which will be in the focus of future studies.

Differentiation and characterization of bone marrow-derived MSCs

Bone marrow-derived MSCs were plated at a density of $1x10^4$ cells per well in 96-well plates (Greiner Bio-one, Kremsmünster, Austria) and subsequently cultivated in the respective differentiation media, i.e., StemMACS™ AdipoDiff for adipogenic or StemMACS™ OsteoDiff (both Miltenyi Biotech, Bergisch Gladbach, Germany) for osteogenic differentiation, respectively, with weekly medium changes. After 3 weeks, samples of MSCs were fixed in 4% paraformaldehyde for 10 min at room temperature (RT). For evaluation of adipogenic differentiation, fixed MSCs were stained with a freshly prepared 60% Red Oil O (Sigma-Aldrich Chemie Gmbh, Munich, Germany) working solution solved in ddH_2O (stock solution: 0.3% Red Oil O solved in 100% isopropanol) for 15 min at RT and washed with 60% isopropanol. Lipid droplets were analyzed via microscopy. For evaluation of osteogenic differentiation, fixed MSCs were stained with 0.5% Alizarin Red (Sigma Aldrich, St. Louis, USA) dissolved in H_2O_{dd} for 15 min at RT to visualize calcium deposition via microscopy (Fig. S1[1]).

Immunophenotyping of bone marrow-derived MSCs via the expression profile of typical surface markers (CD73+, CD90+, CD105+; CD34-, CD45-, CD20-, CD14-, HLA-DR-) was conducted using the MSC Phenotyping Kit (Miltenyi Biotech, Bergisch Gladbach, Germany) according to the manufacturer's instructions (Fig. S2[1]).

Only cell cultures that fulfilled the minimal criteria for MSCs set by the Mesenchymal and Tissue Stem Cell Committee of the International Society for Cellular Therapy (Dominici et al., 2006), including differentiation towards adipogenic and osteogenic lineage and expression of the respective surface marker profile (Fig. S1 and S2[1]), were used for the experiments.

Generation of 3D in vitro *FH models*

To generate the *in vitro* FH models, we firstly isolated, expanded and characterized MSCs before using them in subsequent allogenic combination with human whole blood, which was processed immediately. To this end, 2.5 x 10^5 per well MSCs without any pre-differentiation were centrifuged at 300 g for 3 min at 4°C in a 96-well plate (U-bottom, Greiner Bio one, Kremsmünster, Austria). After discarding the supernatant, the cell pellet was resuspended in 100 µL $CaCl_2$ (10 mM in PBS). 100 µL of allogenic EDTA-blood was added and gently mixed by pipetting. After 30 min of incubation at 37°C, 5% CO_2, the coagulated *in vitro* FH models were transferred into DMEM + GlutaMAX™ supplemented with 10% FCS, 100 units/mL penicillin, 100 mg/mL streptomycin, 0.2% β-glycerophosphate (Sigma Aldrich, St. Louis, USA), 10^{-8} M dexamethasone (Sigma Aldrich, St. Louis, USA) and 0.002% ascorbic acid (Sigma Aldrich, St. Louis, USA), within this study further referred to as osteogenic medium (OM).

For the treatment studies, either 10^{-7} dexamethasone (DEX, impairing fracture healing) or 250 µmol deferoxamine (DFO, promoting fracture healing) was added to the medium. Then, the generated *in vitro* FHs were incubated under either hypoxia (37°C, 5% CO_2 and 1% O_2) or normoxia (37°C, 5% CO_2 and 18% O_2) in a humidified atmosphere for up to 48 h. Hypoxic conditions were achieved using an incubator (Binder, Tuttlingen, Germany) flushed with nitrogen. Normoxic and hypoxic conditions were

[1] doi:10.14573/altex.1910211s

constantly monitored using incubators equipped with CO_2-sensors and O_2-sensors (Binder, Tuttlingen, Germany).

Donor information for the material used in this study is given in Table1. For the flow cytometry analysis, the gene expression analysis and the Bioplex assays in the initial experiments, the blood of blood donors B1-B3 was mixed with either MSC1 or MSC2 (n = 6). For the treatment studies with either DEX or DFO, blood donors B4-B6 were mixed with MSC3 or MSC4 (n = 6).

Preparation of in vitro *FH models for flow cytometry and gene expression analysis*

Immediately after coagulation (0 h = control) or after cultivation for 6, 12, 24 or 48 h in OM, the *in vitro* FH models were washed twice in PBS. Cells were separated using a cell strainer (70 µm, Corning, New York, USA). Erythrocyte lysis was conducted twice at 4°C for 6 min by osmotic shock using erythrocyte lysis buffer (0.01 M $KHCO_3$, 0.155 M NH_4Cl, 0.1 mM EDTA, pH 7.5). Cells were washed in 0.5% BSA in PBS (PBS/BSA).

Flow cytometry analysis

After blocking the unspecific binding of Fc-receptors using a solution containing 5 mg/mL human IgG (IgG1 66.6%, IgG2 28.5%, IgG3 2.7%, IgG4 2.2%; Flebogamma, Grifols, Frankfurt, Germany), cells were washed in PBS/BSA and antibody staining was performed for 15 min on ice using antibodies and dilutions as listed in Table 2. Cells were then washed (PBS/BSA) and centrifuged at 300 g for 3 min in a U-bottom 96-well-plate, supernatants were discarded, and the pellets were resuspended in 0.05% NaN_3 in PBS/BSA (PBS/BSA/Azide). Shortly before analysis, the cells were incubated with 1:25 diluted 7-AAD (BioLegend®, San Diego, USA) for 2 min at RT. Cells were assessed using a MACS Quant Analyzer (Miltenyi Biotech, Bergisch Gladbach, Germany) and evaluated using FlowJo software (Tree Star, USA). The gating strategy is depicted in Fig. S3[1].

Gene expression analysis

Total RNA was extracted using the Arcturus™ PicoPure™ RNA Isolation Kit (Applied Biosystems, Foster City, USA) according to the manufacturer's instructions. cDNAs were synthesized by reverse transcription using the Sensiscript® Reverse Transcription Kit (QIAGEN GmbH, Hilden, Germany) according to the manufacturer's instructions. cDNAs were stored at -20°C until further processing. Quantification of gene expression was performed by qPCR using the DyNAmo Flash SYBR Green qPCR Kit (Thermo Fisher, Waltham, USA) according to the manufacturer's instructions and assessed in a Stratagene Mx3000P (Agilent Technologies, California, USA) using the following program: initial denaturation, 7 min at 95°C; amplification, 45 cycles with 5 s at 95°C, 7 s at 60°C and 9 s at 72°C; melting curve analysis, stepwise temperature increase from 50°C to 95°C every 30 s. Data were normalized to the expression of elongation-factor 1-α (*EF1A*) using the ΔCt-method. We used *EF1A* because of its stable expression in MSCs under conditions of inflammation (involving immune cell activation and morphological changes), hypoxia, and in different cell types (peripheral immune cells) under different drug treatments (Curtis et al., 2010). We excluded several typical house-keeping genes such as glyceraldehyde-3-phosphate dehydrogenase (GAPDH) or β-actin (ACTB) as these are well known to be regulated under hypoxic conditions and after immune cell activation, respectively (Foldager et al., 2009). All primers were purchased from TIB Molbiol (Berlin, Germany) and are listed in Table 3.

Cytokine and chemokine quantification

Supernatants of the *in vitro* FHs were immediately frozen after 48 h and stored at -80°C. The concentrations (pg/mL) of cytokines and chemokines were determined using a multiplex suspension assay (Bio-Rad Laboratories, München, Germany) according to the manufacturer's description. The following cytokines and chemokines (lower detection limit) were measured: IL-1β (7.55 pg/mL), IL-2 (18.99 pg/mL), IL-4 (4.13 pg/mL), IL-5 (20.29 pg/mL), IL-6 (25.94 pg/mL), IL-7 (16.05 pg/mL), IL-8 (37.9 pg/mL), IL-10 (37.9 pg/mL), IL-13 (7.21 pg/mL), IL-17 (24.44 pg/mL), interferon-gamma (IFNγ, 56.32 pg/mL), tumor necrosis factor-alpha (TNFα, 59.53 pg/mL), monocyte chemotactic protein-1 (MCP-1, 27.02 pg/mL), macrophage inflammatory protein MIP-1β (6.27 pg/mL), granulocyte colony-stimulating factor (G-CSF, 50.98 pg/mL), granulocyte-macrophage colony-stimulating factor (GM-CSF, 11.82 pg/mL) and macrophage migration inhibitory factor (MIF, 57.78 pg/mL).

Tab. 2: Antibodies used for the characterization of immune cells and MSCs

Antibody	Marker for	Manufacturer	Catalog Number	Species of origin	Dilution
Monoclonal anti-human CD3	T cells	Miltenyi Biotech	130-113-139	REAfinity™	1:100
Monoclonal anti-human CD4	T helper cells	Miltenyi Biotech	130-113-223	REAfinity™	1:100
Monoclonal anti-human CD8	Cytotoxic T cells	Miltenyi Biotech	130-110-684	REAfinity™	1:100
Monoclonal anti-human CD14	Monocytes	Miltenyi Biotech	130-110-521	REAfinity™	1:100
Monoclonal anti-human CD19	B cells	Miltenyi Biotech	130-113-649	REAfinity™	1:100
Monoclonal anti-human CD45	Pan-Leukocytes	Miltenyi Biotech	130-110-633	REAfinity™	1:50
Monoclonal anti-human CD73	MSCs	BioLegend®	3444004	Mouse	1:20
Monoclonal anti-human CD90	MSCs	BioLegend®	328114	Mouse	1:20

Tab. 3: Primers used

Gene symbol	Gene name	Forward primer	Reverse primer
SPP1	Secreted phosphoprotein 1	GCCGAGGTGATAGTGTGGTT	TGAGGTGATGTCCTCGTCGTCTG
VEGFA	Vascular endothelial growth factor A	AGCCTTGCCTTGCTGCTCTA	GTGCTGGCCTTGGTGAGG
RUNX2	Runt-related transcription factor 2	TTACTTACACCCCGCCAGTC	TATGGAGTGCTGCTGGTCTG
EF1A	Elongation factor 1-alpha	GTTGATATGGTTCCTGGCAAGC	TTGCCAGCTCCAGCAGCCT
MMP2	Matrix metalloproteinase-2	GATACCCCTTTGACGGTAAGGA	CCTTCTCCCAAGGTCCATAGC
IL8	Interleukin 8	GGACCCCAAGGAAAACTGG	CAACCCTACAACAGACCCACAC
IL6	Interleukin 6	TACCCCCAGGAGAAGATTCC	TTTTCTGCCAGTGCCTCTTT
PGK1	Phosphoglycerate kinase 1	ATGGATGAGGTGGTGAAAGC	CAGTGCTCACATGGCTGACT
LDHA	Lactate dehydrogenase A	ACCCAGTTTCCACCATGATT	CCCAAAATGCAAGGAACACT
MMP9	Matrix metalloproteinase-9	CCTGGAGACCTGAGAACCAATC	CCACCCGAGTGTAACCATAGC
HIF1A	Hypoxia-inducible factor 1-alpha	CCATTAGAAAGCAGTTCCGC	TGGGTAGGAGATGGAGATGC

For the dexamethasone and DFO treatment experiments, we set the values of cytokines/chemokines that were not detectable in the samples to the values of the corresponding detection limit.

Statistical analysis

Statistical analysis was conducted using GraphPad Prism (Version 7, La Jolla, USA). The gene expression and Bioplex data are given as mean ± SEM. Flow cytometry data are given as median ± range. All data sets were tested for normal distribution. Since the data sets were not normally distributed, non-parametric tests were performed. Differences between the time points were compared using the Mann Whitney U test. Differences between normoxia and hypoxia or hypoxia vs. dexamethasone/DFO treatment were compared using the Wilcoxon signed rank test (*$p < 0.05$, **$p < 0.01$, ***$p < 0.005$, ****$p < 0.0001$).

3 Results

3.1 Temporal cellular composition of the *in vitro* FH models is dominated by long-term survival of MSCs

In order to simulate the first phase of fracture healing *in vitro*, we generated *in vitro* FH models consisting of human MSCs and peripheral blood cells. Here and in the following experiments, we only used cells meeting the minimal criteria for MSCs set by the Mesenchymal and Tissue Stem Cell Committee of the International Society for Cellular Therapy (Dominici et al., 2006), shown in Figure S1 and S2[1], which guarantees the consistent quality of the MSCs in the various tests performed.

In consideration of mimicking the fracture gap microenvironment characterized by hypoxia and to evaluate its impact on temporal distribution and cell composition, we incubated the *in vitro* FH models for 6, 12, 24 and 48 h under hypoxic conditions (1% O_2, which is the average oxygen level measured in the incubator at 5% CO_2 and high humidity flushed with nitrogen) as compared to normoxia (18% O_2, which is the average oxygen level measured in the incubator at 5% CO_2 and high humidity flushed with room air) (Fig. 1).

Using flow cytometry, we observed a more severe but not significant continuous decline in the frequency of living cells after an incubation period of 48 h under hypoxia (45 ±4%) as compared to normoxia (55 ±3%; Fig. 1A). More in detail, the frequency of innate and adaptive immune cells decreased constantly under hypoxic and normoxic conditions (Fig. 1B). Interestingly, the frequencies of cells representing the adaptive immune response, namely T helper cells (CD45+/CD3+/CD4+), cytotoxic T cells (CD45+/CD3+/CD8+), and B cells (CD45+/CD19+) significantly decreased at 48 h under hypoxic as compared to normoxic incubation. In contrast, cells of the innate immune response, such as granulocytes (CD45+/SSChigh), which were the most abundant cell population until 24 h (25 ±4%), and monocytes (CD45+/SSCintermediate/CD14high), did not differ in their frequencies with regard to oxygen availability.

The frequency of MSCs (CD45-/CD90+/CD73+) within the *in vitro* FH models constantly increased over time, becoming the most abundant cell population with approximately 20% after 48 h of incubation. Interestingly, this effect was even more pronounced under hypoxic conditions, particularly after 48 h, where the frequency of MSCs within the *in vitro* FH models was significantly higher under hypoxic compared to normoxic conditions (23 ±4% vs. 13 ±4%). Thus, hypoxic incubation reduced the frequency of cells of the adaptive immune response and increased the frequency of MSCs, the precursors of chondrocytes and osteoblast/osteocytes important for bone healing.

3.2 Gene expression profile reveals the upregulation of markers relevant for fracture healing in the *in vitro* FH models

With the intention to analyze the impact of hypoxia – most prominent at 48 h – on a selected gene expression pattern, we investigated the expression of marker genes for osteogenesis (*RUNX2, SPP1*), angiogenesis (*VEGFA, IL8, MMP2, MMP9*), inflamma-

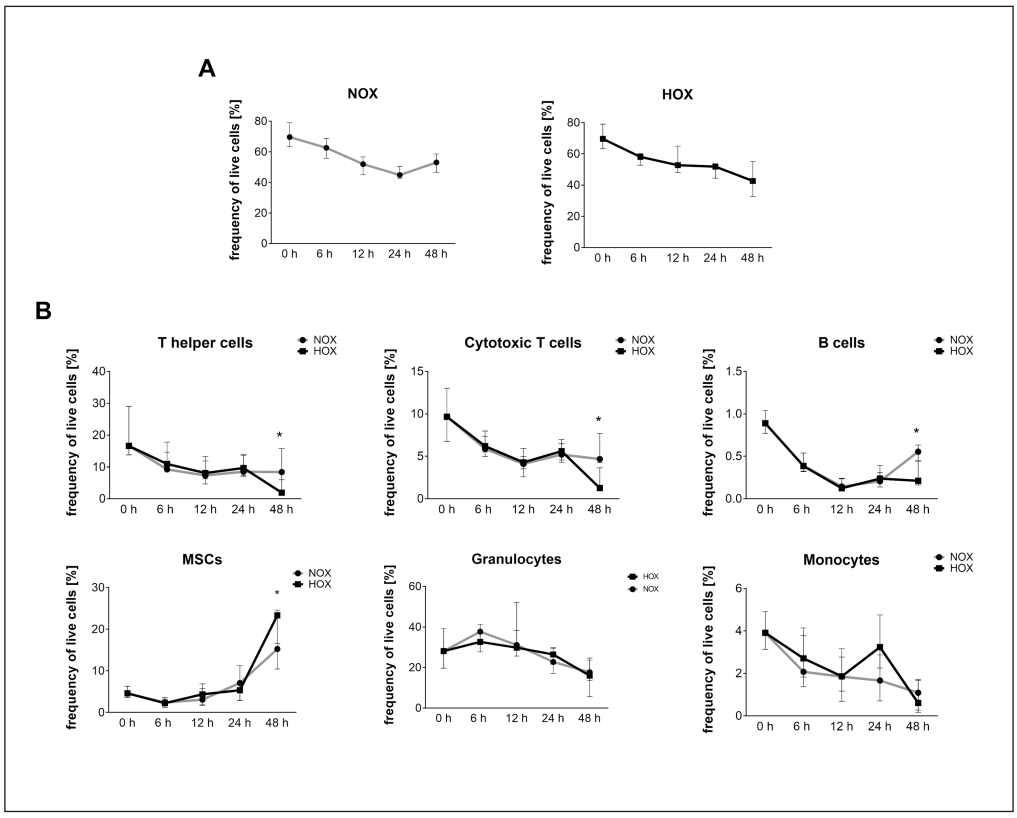

Fig. 1: Hypoxia favors survival of MSCs while T- and B-cell fractions are significantly decreased
(A) Frequency of total cells negative for 7-AAD in the FH cultured in osteogenic differentiation medium under normoxic (NOX; 18% O_2) or hypoxic conditions (HOX; 1% O_2) for 6, 12, 24 and 48 h (median ± range, n = 6). (B) Frequency of immune cell populations (granulocytes, CD14+ monocytes, CD4+ T cells, CD8+ T cells, CD19+ B cells) and MSCs (CD73+, CD90+, CD45-, CD14-) negative for 7-AAD in the *in vitro* FHs cultured in osteogenic differentiation medium under normoxic or hypoxic conditions for 6, 12, 24 and 48 h (median ± range, n = 6). Statistical analysis was conducted using the Wilcoxon signed ranked test (*p < 0.05).

tion (*SPP1, IL6, IL8*), migration (*CXCR4, MMP2, MMP9*), and hypoxic adaptation (*HIF1A, LDHA, PGK1*) of *in vitro* FH models incubated in OM under hypoxic or normoxic conditions for 48 h (Fig. 2). Although, we also investigated the gene expression for the time points 0, 6, 12 and 24 h (Fig. S41), we here focus on the effects after 48 h of incubation. Almost all levels of analyzed marker genes demonstrated a significant hypoxia-mediated induction at 48 h as compared to 0 h except for *IL6, HIF1A*, and *PGK1*. Moreover, compared to normoxic incubation, only *CXCR4* and *IL8* were not significantly induced under hypoxic incubation at this time point.

More in detail, the osteogenic markers, namely the transcription factor *RUNX2* as well as *SPP1*, were significantly up-regulated after 48 h of incubation under hypoxic conditions as compared to 0 h ($p_{RUNX2} = 0.006$, $p_{SPP1} < 0.0001$) (Fig. 2A). Only *SPP1*, but not *RUNX2*, was significantly induced after 48 h incubation under normoxic conditions ($p_{SPP1} < 0.0001$). Both osteogenic marker genes demonstrated a significant increase in gene expression under reduced oxygen availability ($p_{RUNX2} = 0.023$, $p_{SPP1} = 0.009$).

The angiogenic marker *VEGFA* was significantly up-regulated after 48 h incubation under hypoxia ($p_{VEGFA} = 0.0003$) but not under normoxia as compared to 0 h (Fig. 2B). Furthermore, *VEGFA* was significantly up-regulated after 48 h as compared to incubation under normoxic conditions ($p_{VEGFA} = 0.0049$). The pro-inflammatory and pro-angiogenic *IL8* was significantly up-regulated under hypoxia when compared to normoxia ($p_{IL8} = 0.0017$), with no significant alterations in expression after 48 h incubation under normoxic conditions when compared to 0 h (Fig. 2B). In contrast, IL6 gene expression, which is well-known to be induced under inflammatory conditions, was significantly lowered after 48 h incubation under normoxic ($p_{IL6} = 0.0138$) conditions but remained unaltered after 48 h incubation under hypoxic conditions, resulting in a significantly higher expression under hypoxic compared to normoxic conditions after 48 h of incubation ($p_{IL6} = 0.03$; Fig. 2B).

The *CXCR4* transcript encodes the information of the receptor for stromal cell derived factor 1 (SDF-1), which is well-known to facilitate migration of a variety of cell types, including the recruitment of MSCs, towards the fracture site. The expression of *CXCR4* was significantly induced after 48 h compared to 0 h irrespective of oxygen availability ($p_{normoxia} = 0.005$; $p_{hypoxia} = 0.002$; Fig. 2C). Moreover, gene expression of *MMP2* and *MMP9*, encoding for matrix metalloproteinases and important for vascularization and migration, were significantly up-regulated after 48 h as compared to 0 h under hypoxic but not under normoxic conditions ($p_{MMP2} = 0.0197$, $p_{MMP9} = 0.002$; Fig. 2C). Both genes were significantly more highly expressed when comparing normoxia vs hypoxia ($p_{MMP2} = 0.0244$, $p_{MMP9} = 0.0137$).

Typical markers for cellular adaptation towards hypoxia (*LDHA*, *PGK1*, and *HIF1A*) were significantly more highly expressed after 48 h of incubation under hypoxic when compared to normoxic conditions ($p_{LDHA} = 0.008$, $p_{PGK1} = 0.031$, $p_{HIF1A} = 0.027$; Fig. 2D). While *LDHA* was also significantly up-regulated after 48 h of incubation under hypoxia but not normoxia compared to 0 h ($p = 0.0002$), PGK1 demonstrated a trend towards an increased

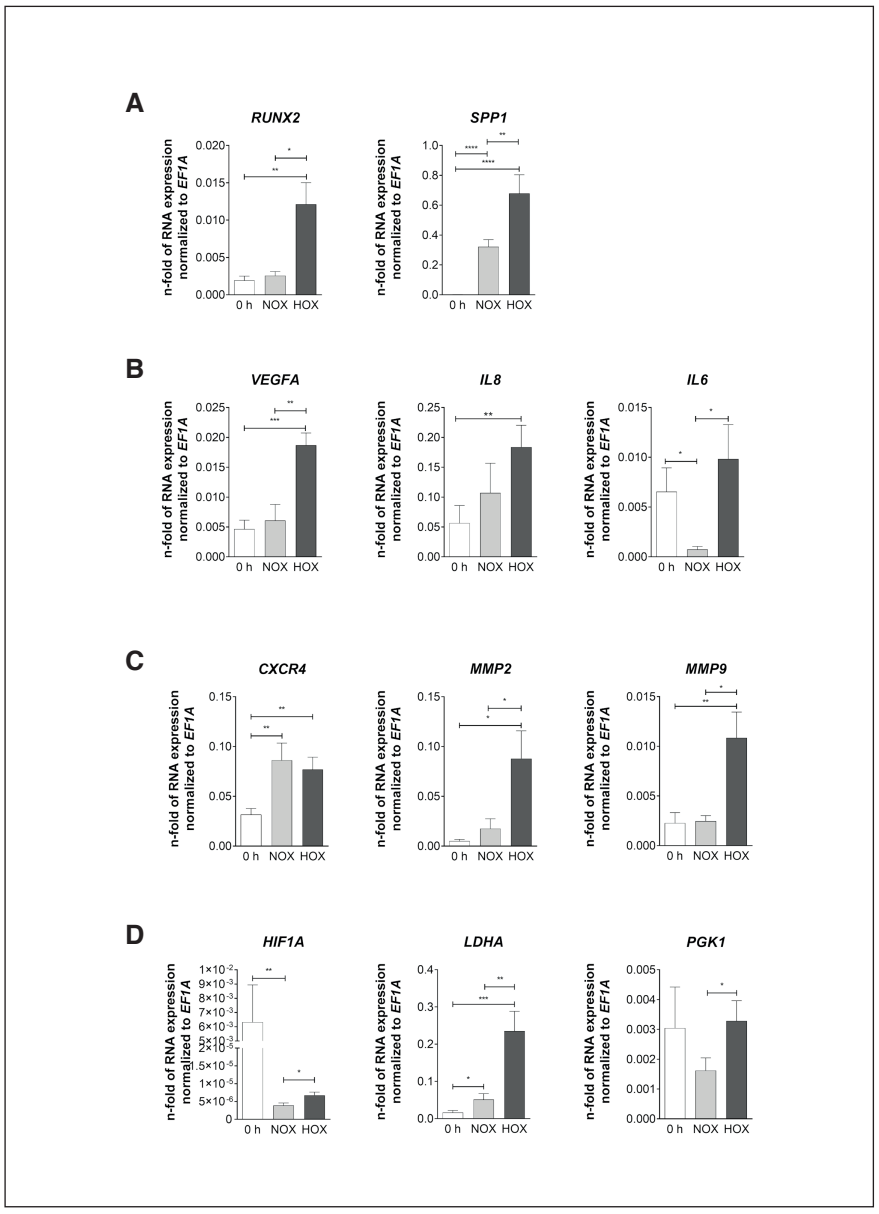

Fig. 2: Osteogenic, angiogenic, inflammatory, migration and metabolic markers are significantly upregulated after 48 h of incubation, more pronounced under hypoxia, in FHs
Relative gene expression within the *in vitro* FHs after cultivation in OM for 48 h of (A) the osteogenic markers *RUNX2* and *SPP1*, (B) the angiogenic/inflammatory markers *VEGFA*, *IL8*, *IL6*, (C) the migration markers *CXCR4*, *MMP2* and MMP9, and (D) the metabolic markers *HIF1A*, *LDHA* and *PGK1*. The expression is shown at 0 h (white bars) and under normoxia (NOX; light grey bars) or hypoxia (HOX; dark grey bars). All values are normalized to the "housekeeping gene" *EF1A* (mean ± SEM, n = 12). Statistical analysis was conducted using the Mann Whitney U test to compare the values to 0 h, and the Wilcoxon signed rank test to compare normoxia and hypoxia (*$p < 0.05$, **$p < 0.01$, ***$p < 0.001$, ****$p < 0.0001$).

expression ($p = 0.086$) and *HIF1A* showed a decrease for both normoxia and hypoxia.

Taken together, almost all markers of gene expression that are important for proper fracture healing demonstrated a significant hypoxia-mediated induction after 48 h.

3.3 Hypoxia does not significantly impact cytokine/chemokine levels in the supernatant of *in vitro* FH models

In order to confirm the gene expression pattern of pro-angiogenic and pro-inflammatory markers after 48 h incubation and to characterize the secretion of cytokines and chemokines, we analyzed the respective supernatants. While IL-1β, IL-2, IL-4, IL-5, IL-7, IL-10, IL-13, IL-17, TNFα and IFNγ were not detectable in the supernatants of the *in vitro* FH models, certain levels of the pro-inflammatory IL-6, pro-inflammatory and pro-angiogenic MIF and the pro-inflammatory and pro-angiogenic IL-8 as well as the chemoattractant protein MCP-1 and the pro-inflammatory G-CSF and GM-CSF were detected (Fig. 3). IL-6 and IL-8 were detectable in the medium after 48 h incubation under both normoxia and hypoxia, with a trend to a higher level in the latter ($p_{IL\text{-}6} = 0.094$, $p_{IL\text{-}8} = 0.063$), while MIF, MCP-1, G-CSF and GM-CSF levels were comparable irrespective of oxygen availability.

3.4 Dexamethasone favors the survival of immune cells over MSCs, suppresses osteogenesis and enhances the secretion of inflammatory cytokines

To determine whether the *in vitro* FH model is suitable to reflect the known glucocorticoid-mediated disturbance of the initial healing phase, we analyzed the impact of the glucocorticoid dexa-

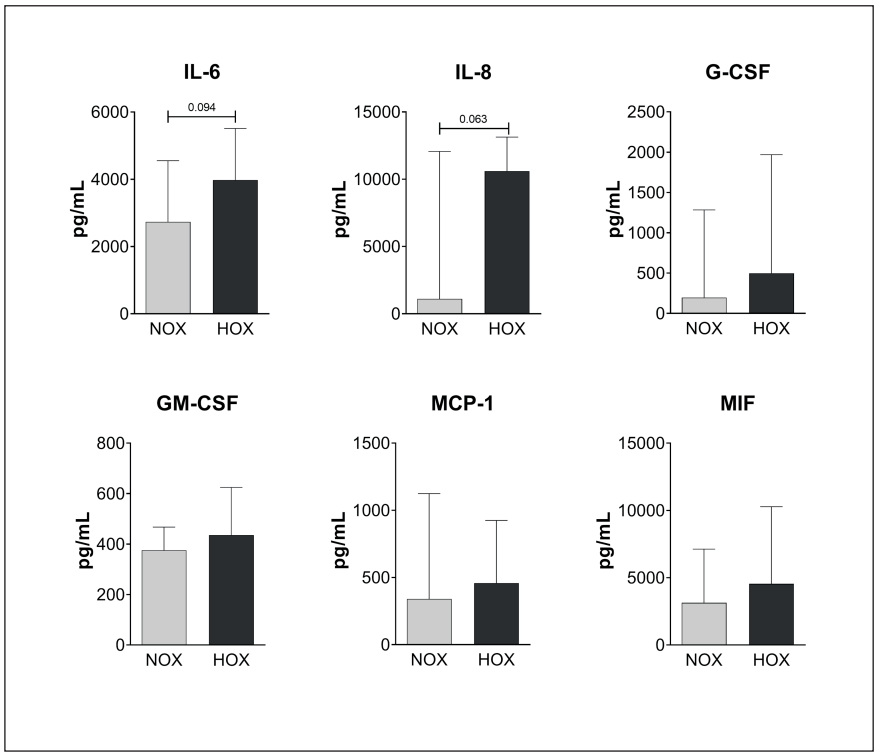

Fig. 3: Induction of angiogenic as well as pro-inflammatory cytokines/ chemokines in FHs

In vitro FHs were incubated under normoxia (NOX) or hypoxia (HOX) for 48 h in osteogenic medium, and the concentration of cytokines and chemokines was measured in the supernatant. Values represent median ± range (n = 6) of secreted protein (pg/mL) in the supernatant. Statistical analysis via Wilcoxon signed rank test. p values indicate statistical trends ($p < 0.1$).

methasone (DEX) at a clinically relevant dose of 10^{-7} M under physiological conditions (under hypoxia and in a pro-osteogenic environment) after 48 h of incubation as compared to the untreated control. Surprisingly, DEX treatment diminished the frequency of living cells within the *in vitro* FH models to a lesser extent than the corresponding control (Fig. 4A). Upon closer analysis, DEX significantly reduced the frequency of MSCs while increasing the proportions of all immune cell populations analyzed, leading to an enrichment of the granulocyte population (25 ±4%) within the DEX-treated *in vitro* FH models. In line, gene expression analysis demonstrated that the expression of osteogenic marker genes (*RUNX2, SPP1*) was significantly diminished in the FH models after treatment with DEX as compared to the untreated control (Fig. 4B). Similarly, the gene expression of pro-inflammatory *IL6* and *CXCR4* was significantly reduced in the DEX-treated FH models. However, DEX treatment influenced neither the expression of pro-angiogenic genes (*VEGFA, IL8*) nor genes involved in the adaptation towards hypoxia (*PGK1, LDHA*, and *HIF1A*). Of note, under normoxic cultivation conditions, DEX abolished osteogenic differentiation while inducing lipid droplet formation only at a high concentration of 10^{-5} M DEX but not at the clinically relevant dose of 10^{-7} M (Fig. S7[1]).

Focusing on the release of cytokines and chemokines after DEX treatment under hypoxic conditions, we detected IL-4, IL-6, IL-8, IL-17, IFNγ, TNFα, G-CSF, GM-CSF, MIF and MCP-1 in considerable amounts in the supernatant of *in vitro* FH models (Fig. 4C). Interestingly, all factors detected demonstrate a higher abundance in the supernatant of *in vitro* FH models treated with DEX but remained low in the untreated controls.

3.5 Chemical induction of hypoxia using DFO does not fully mimic hypoxic conditions created in a hypoxia-incubator

DFO has been widely reported to increase fracture-healing properties by supporting HIF-mediated angiogenesis and osteogenesis independent of species, model and evaluation methods (Donneys et al., 2013a,b, 2015, 2016; Drager et al., 2016, 2017; Farberg et al., 2012; Guzey et al., 2016; Matsumoto and Sato, 2015; Shen et al., 2009; Stewart et al., 2011; Yao et al., 2016; Zhang et al., 2012; Kang et al., 2016; Kusumbe et al., 2014; Li et al., 2015; Liu et al., 2014; Wang et al., 2017b). To simulate the clinical application of DFO to overcome an inadequate hypoxic response in patients that are prone to delayed healing, we treated the *in vitro* FH models with 250 µM DFO under normoxic conditions (Fig. 5) or left them untreated (for comparison, treatment under hypoxic conditions is shown in Fig. S5[1]).

Focusing on the frequencies of total live cells (Fig. 5A), we did not observe any difference after treatment with DFO as compared to the normoxic untreated control *in vitro* FH models. Interestingly, the frequency of the individual cell populations displayed a significantly reduced frequency of T cells after DFO treatment. Both the frequency of T helper cells as well as the frequency of cytotoxic T cells significantly declined upon DFO treatment in the *in vitro* FH models (10 ±3% to 7 ±2% and 5,5 ±1% to 4 ±1%; $p = 0.03$). Conversely, the proportion of granulocytes was significantly higher in the DFO-treated group (28 ±3%) compared to the normoxic control group (18 ±2%; $p = 0.03$). No other cell population analyzed demonstrated considerable differences between both conditions.

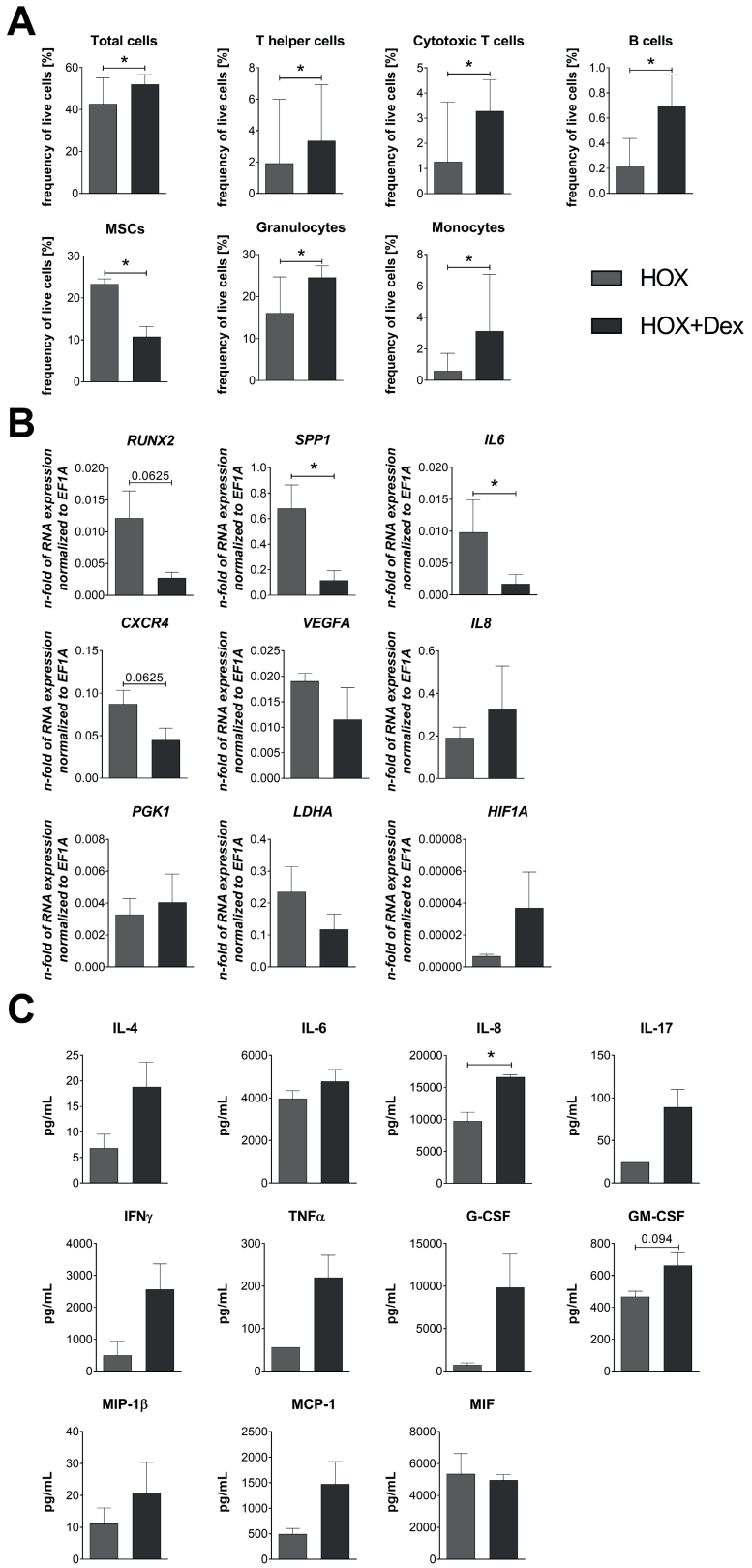

Fig. 4: Dexamethasone favors the survival of immune cells over MSCs, suppresses osteogenesis, and enhances the secretion of inflammatory cytokines

In vitro FHs were incubated under hypoxia (HOX) in the presence or absence of 10^{-7} M dexamethasone (Dex) for 48 h in OM. (A) Frequency of total cells and individual cell populations negative for 7-AAD, (B) relative gene expression of relevant genes normalized to *EF1A*, and (C) concentration of secreted protein (pg/mL) in the supernatant (C). Values represent the median ± range (n = 6) for the cell composition analysis and the mean ± SEM (n = 6) for the gene expression and the secreted proteins. Statistical analysis was conducted using the Wilcoxon signed rank test (*$p < 0.05$).

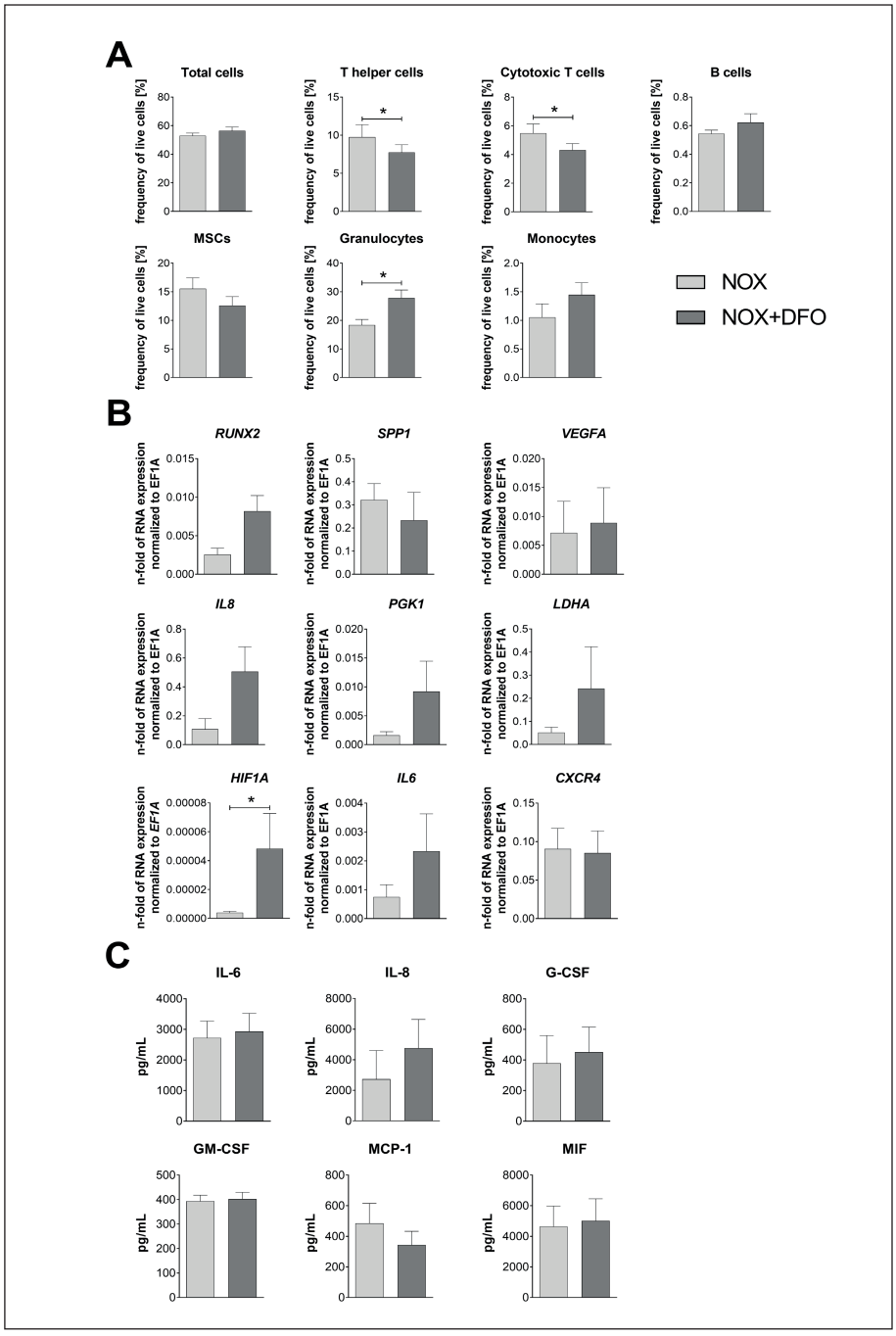

Fig. 5: DFO significantly increases the frequency of granulocytes, decreases the frequency of T cells, and enhances the expression of hypoxia-related and inflammatory markers

In vitro FH models were incubated under normoxia (NOX) in the presence or absence of 250 μM DFO for 48 h in osteogenic medium. (A) Frequency of total cells and individual cell populations negative for 7-AAD, (B) relative gene expression of relevant genes normalized to *EF1A*, and (C) concentration of secreted protein (pg/mL) in the supernatant (C). Values represent the median ± range (n = 6) for the cell composition analysis and the mean ± SEM (n = 6) for the gene expression and the secreted proteins. Statistical analysis was conducted using the Wilcoxon signed rank test (*$p < 0.05$).

Regarding the gene expression pattern (Fig. 5B), we observed a greater expression of the early osteogenic transcription factor *RUNX2* ($p = 0.06$) and the inflammatory markers *IL6* (0.1) and *IL8* ($p = 0.06$) after treatment with DFO compared to the control group. Additionally, genes involved in the adaptation to hypoxic conditions were more highly expressed in the group treated with DFO compared to the corresponding normoxic controls ($p_{PGK1} = 0.04$, $_{pHIF1A} = 0.03$). Generally, the treatment with DFO did not lead to a significantly higher cytokine/chemokine release compared to normoxia (Fig. 5C).

4 Discussion

In order to provide a pre-clinical model of the initial healing phase, we established an *in vitro* FH model based on human cells that can be used (i) to investigate cellular mechanisms and adaptive processes during the initial phase of fracture healing, (ii) to identify new potential therapeutic targets, and (iii) to determine the efficacy and effectiveness of therapeutics for the treatment of fracture healing disorders (iv) to effectively reduce the number of animal experiments.

Mimicking the *in vivo* situation of the fracture gap by applying a hypoxic microenvironment, we observed a predominant reduction in the frequency of adaptive immune cells and an increase in the frequency of MSCs (Fig. 1). Of note, the trauma-induced rupture of blood vessels opens the bone channel and forms a hematoma of clotted bone marrow/blood, consisting mostly of immune cells, their precursors, and endothelial and stromal cells, which initiates the cascade of bone regeneration by further recruitment of immune cells and MSCs (Knight and Hankenson, 2013).

While the importance of MSCs as precursors of chondrocytes and bone cells (osteoblasts and osteocytes) (Knight and Hankenson, 2013; Kolar et al., 2011; Hoff et al., 2016) and as terminators of the inflammatory phase, resembling the *in vivo* situation (Kolar et al., 2011), is undisputed, the role of immune cells such as granulocytes, T and B cells remains controversial (Kovtun et al., 2016; Grogaard et al., 1990; El Khassawna et al., 2017; Konnecke et al., 2014; Reinke et al., 2013; Toben et al., 2011). Although generally, cells rich in mitochondria often have an intrinsic need for sufficient oxygen supply and are barely able to cope with hypoxic conditions (e.g., neuronal cells), the survival capacity and activation status of immune cells (T cells, B cells, monocytes, neutrophils) is enhanced under hypoxic conditions, mainly due to activation/stabilization of the HIF-signaling pathway in an oxygen-restricted environment (Krzywinska and Stockmann, 2018). In terms of MSCs, hypoxia seems to favor MSC survival and their differentiation towards the chondrogenic and osteogenic lineages once differentiation is induced, while adipogenesis is reduced (Wagegg et al., 2012; Lee et al., 2016). However, whether inflammatory cells and MSCs actually differ in their tolerance of oxygen is still a matter of research.

Using RAG1-deficient mice, which lack an adaptive immune system, Toben et al. (2011) demonstrated enhanced fracture healing due to accelerated endochondral ossification and a shift from pro-inflammatory to anti-inflammatory cytokines (Toben et al., 2011). Moreover, depletion of only CD8+ T cells also enhanced/accelerated fracture healing in a mouse osteotomy model, indicating a possible contribution of adaptive immune cells to delayed or disturbed fracture healing (Reinke et al., 2013; Toben et al., 2011). Nevertheless, T and B cells evidently contribute to a higher bone quality in the later stages of fracture healing by facilitating the collagen organization process (El Khassawna et al., 2017; Konnecke et al., 2014). However, granulocytes, which are responsible for the removal of dead cells and cell debris in the very initial phase after trauma (Soehnlein et al., 2009), and which are the most abundant cell fraction in the early FH (Kovtun et al., 2016), provide an "emergency extracellular matrix" for infiltrating stromal cells (Bastian et al., 2016), thereby essentially contributing to proper fracture healing (Kovtun et al., 2016). Although Groogard et al. (1990) did not observe any impact of neutropenia on callus formation in rats, Kovtun et al. (2016) observed diminished bone content, impaired mechanical properties and bone healing after 21 days in fractured mice after using an anti-Ly-6G-antibody to reduce neutrophil numbers. Using patient-derived isolated *ex vivo* FHs, we previously reported a decrease of granulocytes already after 24 h of incubation, which was even more pronounced under hypoxia (Hoff et al., 2013).

In our FH model, we observed an increase in the frequency of MSCs, key players in the initial phase of fracture healing, which generate the precursors of chondrocytes and osteoblast/osteocytes, which are essential for proper bone healing (Knight and Hankenson, 2013; Kolar et al., 2011; Hoff et al., 2016), and are capable of terminating the inflammatory phase (Kolar et al., 2011) by inhibition of immune cell proliferation (Le Blanc et al., 2003; Madrigal et al., 2014; Gieseke et al., 2007; Bocelli-Tyndall et al., 2007; Potian et al., 2003; Kovach et al., 2015), thereby modulating the immune response and conveying immune tolerance (Nauta and Fibbe, 2007). The shift of the cellular distribution to a pattern dominated by MSCs also influences the gene expression pattern in our FH model, demonstrating a significant hypoxia-mediated induction after 48 h, especially for hypoxia response and osteogenic marker gene expression (Fig. 2), while not significantly altering but enhancing inflammatory cytokine and chemokine levels in the supernatant (Fig. 3). The induction of a hypoxia response and osteogenic marker gene expression as well as no further induction of inflammatory cytokine and chemokine levels have been proposed to be important for proper fracture healing (Hoff et al., 2011).

Focusing on the gene expression pattern under hypoxic incubation conditions, we could successfully mimic the situation in the fracture gap by confirming the findings observed in hematomas derived from 40 patients obtained between 48 and 72 h after surgery (Kolar et al., 2011) as summarized in Table 4. Additionally, in this study we confirmed that hypoxia promotes osteogenesis of MSCs as reported previously (Haque et al., 2013; Wagegg et al., 2012; Lennon et al., 2001). Moreover, we observed secretion of pro-angiogenic (IL-8) and pro-inflammatory cytokines/chemokines (IL-6, G-CSF, GM-CSF, and MCP), factors well-known to be responsible for the recruitment and activation of leukocytes in an inflammatory milieu, after incubation for 48 h under both normoxia and hypoxia (Fig. 3), confirming the findings of our previous study using hematomas derived from 40 patients (Hoff et al., 2016). Unexpectedly, we could not observe a relevant amount of the early inflammatory markers TNFα and IL-1β. However, Granero-Molto et al. (2009) also reported decreased secretion of TNFα and IL-1β after transplanting MSCs into the fracture gap using a stabilized tibia fracture mouse model.

Although our FH model has some limitations with regard to the completeness of cell types involved, we could demonstrate a decrease in the frequency of lymphocytes and an increase in the frequency of MSCs after 48 h of incubation under hypoxic conditions, suggesting the capacity of MSCs to restrict the initial inflammatory phase of fracture healing while initiating osteochondral differentiation.

For technical reasons, we combined peripheral blood and MSCs from different donors (allogenic combination), as the MSCs were cultured for some weeks before being combined with fresh blood. We considered this unproblematic as MSCs have been characterized as immune-privileged, immune evasive (Ankrum et al., 2014) and/or, in some conditions, immunosuppressive (e.g., in case of T cell proliferation). However, the activation of immune cells via allogenic MSCs is still controversially discussed as previously reviewed in detail (Hare et al., 2012; Rozier et al., 2018; Zhang et al., 2015). Here, we observed that

T cells in combination with allogenic MSCs remained quiescent with regard to the expression of the early activation marker CD69 and the late activation marker CD25 (Fig S6[1]). The observed restriction of inflammation may underline the well-known therapeutic benefit of allogenic MSC transplants, which have no obvious disadvantages compared to autologous MSC transplantation (Rozier et al., 2018).

Finally, we compared the established *in vitro* FH model to *ex vivo* data from primary human FHs obtained between 48 and 72 h after trauma and found profound similarities with regard to data from flow cytometry, gene expression and cytokine secretion (Tab. 4 and 5). Interestingly, we also found similar trends with regard to the cell composition, gene expression pattern and the effects of hypoxia after 48 h of incubation in an equine *in vitro* FH model (Pfeiffenberger et al., 2019).

In order to further validate the applicability of the *in vitro* FH model for drug testing, we treated the *in vitro* FHs with either DEX (impairs fracture healing) or DFO (supports fracture healing), in order to mimic either impaired or supported bone healing processes during the initial phase of fracture healing (Fig. 4 and 5).

DEX belongs to the wide class of glucocorticoids that significantly improve the quality of life of many patients suffering from diseases caused by a dysregulated immune system based on their strong immunosuppressive, anti-inflammatory and anti-allergic effects on immune cells, tissues and organs (Strehl et al., 2019). However, glucocorticoids are also known to influence bone metabolism by inhibiting bone formation, enhancing bone resorption and impairing adequate bone healing (Canalis, 2003; Frenkel et al., 2015; Sato et al., 1986; Sawin et al., 2001; Waters et al., 2000). Here, we incubated the *in vitro* FH models with a therapeutic dose of 10^{-7} M DEX for 48 h under pathophysiologic hypoxia. Upon treatment with DEX, we observed a significantly lower frequency of MSCs and significantly higher frequencies of immune cells, suppressed osteogenic gene expression (*RUNX2*, *SPP1*), and enhanced secretion of inflammatory cytokines (Fig. 4). Although DEX is well-known to induce apoptosis, particularly in T cells, and suppresses T cell activation (Xing et al., 2015), during co-incubation of MSCs and immune cells (e.g., PBMCs), DEX has been reported to enhance immune cell proliferation and reverse the immunosuppressive effect of MSCs (Chen et al., 2014; Buron et al., 2009). Regarding the latter finding, DEX has been shown to even reverse the anti-inflammatory effect of transplanted MSCs as shown by Chen et al. (2014) in a mouse model of liver cirrhosis. Furthermore, *in vitro* osteoblastic differentiation is delayed by treatment with DEX (Canalis, 1996) as indicated also in the *in vitro* FH model by a reduced osteogenic gene expression (*RUNX2*, *SPP1*). We and others have also reported that DEX suppresses hypoxia-induced HIF-target gene expression (Wu et al., 2014; Gaber et al., 2011), which could be confirmed in the *in vitro* FH model based on reduced gene expression of *VEGFA*, *LDHA*, and *CXCR4*. Although, DEX is well-known to suppress inflammation (Strehl et al., 2019), we observed an enhanced secretion of inflammatory cytokines, which may lead to delayed or disturbed bone healing as suggested from *ex vivo* patient-derived data (Hoff et al., 2011). Indeed, Liu et al. (2018) demonstrated that glucocorticoids delayed fracture healing and impaired bone biomechanical properties in mice. Taken together, the effects of DEX within our model may resemble the processes of delayed or impaired fracture healing.

In contrast to DEX, DFO has been reported to support angiogenesis (Farberg et al., 2014), to enhance the vascular response to fractures (Donneys et al., 2012), and to augment the restoration and mineralization of the callus (Donneys et al., 2013a), making it an attractive off-label therapeutic target with regard to fracture healing. Additionally, DFO stabilizes HIF-1α by suppressing the oxygen-sensitive prolyl hydroxylases (PHDs), which are responsible for the tagging of HIF-1α for proteasomal degradation, thereby mimicking hypoxic conditions and markedly improving osteogenesis (Qu et al., 2008) and bone regeneration (Wan et al., 2008). To simulate the clinical application of DFO to overcome an inadequate hypoxic response in patients that are prone to delayed healing as demonstrated previously (Kolar et al., 2011), we treated the *in vitro* FH models with 250 µM DFO under normoxic conditions (Fig. 5) or left them untreated (treatment under hypoxic conditions are shown in Fig. S5[1]). Here, we used DFO as a hypoxia mimicking agent to overcome a delay or failure of the cells to adapt to hypoxic conditions, which we simulated using normoxic incubation conditions. As a result, we observed that the frequency of T helper cells as well as of cytotoxic T cells (Fig. 5) was diminished when treated with DFO compared to normoxia, while the frequency of granulocytes was significantly higher. This finding can be explained by an anti-proliferative effect of DFO on activated T lymphocytes, but with barely any effect on granulocytes as demonstrated by Hileti et al. (1995). Similarly, DFO has been demonstrated to diminish proliferation and survival of MSCs (Zeng et al., 2011; Wang et al., 2017a), which may explain the decline in the frequency of MSCs as compared to normoxia in our model. However, as expected, DFO-treatment as well as hypoxia up-regulated *HIF1A*, *PGK1* and *LDHA* as compared to their corresponding controls while only *RUNX2*, which is a very early marker for osteogenic processes, but not *SPP1*, the downstream marker of osteogenesis, was induced by DFO-treatment. With regard to the secretion of cytokines, IL-6 and IL-8 were both similarly secreted, whereas DFO-treatment resulted in scarcely any enhanced secretion of G-CSF, GM-CSF, MCP-1 and MIP-1β compared to normoxia and therefore did not contribute to an enhancement of inflammation as observed for DEX treatment. Although the treatment with DFO could not fully recreate the situation obtained by incubation under hypoxic conditions, DFO enhanced the expression of hypoxia adaptation-relevant genes and pro-osteogenic factors (*RUNX2*), thus promoting cellular adaptation to hypoxic conditions and the pro-osteogenic phenotype of MSCs found in the fracture gap.

Although we were able to mimic key features of the initial phase of fracture healing *in vitro*, the model still has room for improvement. The *in vitro* FH model presented here is under development and still requires optimization and qualification. To optimize the model, we will have to overcome technical challenges that forced us to use an allogenic approach; the optimal model should be derived from autologous and xeno-free material (autologous serum, MSCs and peripheral blood). Furthermore, we

Tab. 4: Gene expression data from our *in vitro* FH model (n = 12, 48 h incubation under hypoxia) and from an *ex vivo* study using primary human fracture hematomas obtained between 48 and 72 h after trauma (n = 40) (Kolar et al., 2011)[a]

Gene symbol	Importance in the fracture healing process	*In vitro* FH model (hypoxia for 48 h)	*Ex vivo* primary human FHs (< 72 h)
RUNX2	Key regulator that directs mesenchymal stromal cells towards the osteoblastic lineage (Vimalraj et al., 2015; Komori, 2010).	↑**	↑
SPP1	Coding gene for osteopontin (OPN) is a differentiation marker for osteoblastic cells induced by hypoxia (Denhardt and Noda, 1998; Sila-Asna et al., 2007; Gross et al., 2005).	↑****	↑*
VEGFA	Most important pro-angiogenic factor (Schipani et al., 2009; Martin et al., 2009; Beamer et al., 2010) essential for the reestablishment of oxygen supply and promotes osteogenesis (Hoff et al., 2016; Grosso et al., 2017).	↑***	↑*
IL8	Responsible for the activation and differentiation of leukocytes in an inflammatory osteogenesis environment (Herman et al., 2008).	↑**	↑***
IL6	Key cytokine in the initial phase of fracture healing (Cassuto et al., 2018).	↑	↑***
CXCR4	Responsible for the homing of MSCs, promotes bone repair (Liu et al., 2013; Yellowley, 2013) and reflects the migratory capacity of immune and stem cells (Campbell et al., 2003; Kunkel and Butcher, 2002).	↑**	↑*
LDHA	(Hypoxia-mediated) marker of induced glycolysis, contributes to acidic pH, HIF-target gene (Semenza, 1998; Gaber et al., 2005).	↑***	↑**
PGK1	(Hypoxia-mediated) marker of induced glycolysis (Semenza, 1998; Gaber et al., 2005).	↓	↑
HIF1A	Master regulator of the adaptation towards a hypoxic microenvironment in a large quantity of different cell types (Semenza, 1998; Gaber et al., 2005) regulated on protein- but not on mRNA-level (Semenza, 1998; Gaber et al., 2005).	↓	↑**
MMP2	Remodeling of extracellular matrix, crucial for the survival of bone cells and vasculogenesis/ angiogenesis and fracture healing (Stamenkovic, 2003; Paiva and Granjeiro, 2017; Varghese, 2006; Cui et al., 2017; Lieu et al., 2011).	↑*	n.a.
MMP9	Remodeling of extracellular matrix, crucial for the survival of bone cells and vasculogenesis/ angiogenesis and fracture healing (Stamenkovic, 2003; Paiva and Granjeiro, 2017; Varghese, 2006; Cui et al., 2017; Colnot et al., 2003).	↑**	n.a.

[a] up-↑ or down-↓ regulation of the genes. *p < 0.05, **p < 0.01, ***p < 0.001, n.a. = not analyzed

Tab. 5: Cell frequencies from our *in vitro* FH model (n = 6, 48 h incubation under hypoxia) and from an *ex vivo* study using primary human fracture hematomas obtained between 48 and 72 h after trauma (n = 40) (Kolar et al., 2011)

Cell type	CD surface marker	*In vitro* FH model (hypoxia for 48 h)	*Ex vivo* primary human FHs (< 72 h)
T cells	CD45+CD3+	3.7% (2.4-10.6%)	8.2% (1.1-39.4%)
T helper cells	CD45+CD3+CD4+	1.9% (1.1-6%)	3.1% (1.4-15.4%)
Cytotoxic T cells	CD45+CD3+CD8+	1.3% (0.9-2.5%)	1.9% (0.2-12.6%)
Monocytes	Scatter and CD45+CD14+	0.6% (0.3-1.7%)	4.9% (0.1-38.5%)
B cells	CD45+CD3-CD19+	0.25% (0.2-0.4%)	0.9% (0.1-5.8%)
MSCs	CD45-CD73+CD90+	23.4% (16.6-24.5%)	n.a.
Granulocytes	Scatter and CD45+ vs. CD16+	16.1% (5.6-24.7%)	64.2% (0.8-94%)
Not assigned cells	n. a.	37.1% (27.6-45.8%)	12.2% (1.2-85.6%)

Frequency of cells (min-max in %). Granulocytes gated *in vitro* via CD45+/ FSC-SSC-gate, *ex vivo* via CD16; n.a., not analyzed

would like to include further cell types present in the bone marrow and in the fracture gap, including hematopoietic stem cells and cells of their subsequent progenitor lineages, endothelial progenitor cells and perivascular cells (Braham et al., 2019). Finally, we wish to implement the model into a perfusion system to provide better nutrient supply and waste removal, which we plan to achieve by using a bioreactor platform. This promises to extend the life-time of our model to allow the study of later phases of bone regeneration.

Prospectively, the established and optimized model will provide the opportunity to (1) study cellular and humoral processes of bone regeneration, (2) investigate the underlying mechanisms of how hypoxic conditions modulate cell survival, proliferation, communication and differentiation during the initial phase of fracture healing, (3) screen for new potential therapeutics and assess their efficacy to support fracture healing and to treat fracture healing disorders, and (4) determine side effects of pharmacological substances.

5 Conclusion

In the study presented here, we developed an *in vitro* human-based FH model using human MSCs and human peripheral blood as a tool for preclinical drug testing. We characterized key mechanisms important for proper fracture healing and demonstrated that hypoxia preferred the survival of MSCs to immune cells. Fracture-healing relevant genes/factors were considerably upregulated after 48 h of incubation, most often significantly enhanced by hypoxia. Additionally, cytokines/chemokines that are crucial during the initial phase of fracture healing were secreted. These findings resemble previous results from our group from an *ex vivo* study using patient-derived FHs. We could highlight significant similarities to human *in vitro*, *ex vivo* and animal-based *in vivo* data. To prove the suitability of our 3D *in vitro* FH model for drug testing, we treated the developed system with DEX or DFO, thereby confirming the responsiveness to commonly used drugs and newly developed therapeutics. We were able to show that both fracture-healing disrupting and fracture-healing promoting substances can influence the *in vitro* FH model in ways similar to what has been observed *in vivo*. Therefore, we conclude that our model is able to correctly mimic human fracture hematoma and could reduce the number of animal experiments in early preclinical studies.

References

Ankrum, J. A., Ong, J. F. and Karp, J. M. (2014). Mesenchymal stem cells: Immune evasive, not immune privileged. *Nat Biotechnol 32*, 252-260. doi:10.1038/nbt.2816

Annamalai, R. T., Turner, P. A., Carson, W. F. 4th et al. (2018). Harnessing macrophage-mediated degradation of gelatin microspheres for spatiotemporal control of BMP2 release. *Biomaterials 161*, 216-227. doi:10.1016/j.biomaterials.2018.01.040

Bagi, C. M., Berryman, E. and Moalli, M. R. (2011). Comparative bone anatomy of commonly used laboratory animals: Implications for drug discovery. *Comp Med 61*, 76-85. https://www.ncbi.nlm.nih.gov/pmc/articles/PMC3060425/pdf/cm2011000076.pdf

Baht, G. S., Vi, L. and Alman, B. A. (2018). The role of the immune cells in fracture healing. *Curr Osteoporos Rep 16*, 138-145. doi:10.1007/s11914-018-0423-2

Bastian, O. W., Koenderman, L., Alblas, J. et al. (2016). Neutrophils contribute to fracture healing by synthesizing fibronectin+ extracellular matrix rapidly after injury. *Clin Immunol 164*, 78-84. doi:10.1016/j.clim.2016.02.001

Beamer, B., Hettrich, C. and Lane, J. (2010). Vascular endothelial growth factor: An essential component of angiogenesis and fracture healing. *HSS J 6*, 85-94. doi:10.1007/s11420-009-9129-4

Bocelli-Tyndall, C., Bracci, L., Spagnoli, G. et al. (2007). Bone marrow mesenchymal stromal cells (BM-MSCs) from healthy donors and auto-immune disease patients reduce the proliferation of autologous- and allogeneic-stimulated lymphocytes in vitro. *Rheumatology (Oxford) 46*, 403-408. doi:10.1093/rheumatology/kel267

Braham, M. V. J., Li Yim, A. S. P., Garcia Mateos, J. et al. (2019). A human hematopoietic niche model supporting hematopoietic stem and progenitor cells in vitro. *Adv Healthc Mater 8*, e1801444. doi:10.1002/adhm.201801444

Buron, F., Perrin, H., Malcus, C. et al. (2009). Human mesenchymal stem cells and immunosuppressive drug interactions in allogeneic responses: An in vitro study using human cells. *Transplant Proc 41*, 3347-3352. doi:10.1016/j.transproceed.2009.08.030

Campbell, D. J., Kim, C. H. and Butcher, E. C. (2003). Chemokines in the systemic organization of immunity. *Immunol Rev 195*, 58-71. doi:10.1034/j.1600-065X.2003.00067.x

Canalis, E. (1996). Clinical review 83: Mechanisms of glucocorticoid action in bone: Implications to glucocorticoid-induced osteoporosis. *J Clin Endocrinol Metab 81*, 3441-3447. doi:10.1210/jcem.81.10.8855781

Canalis, E. (2003). Mechanisms of glucocorticoid-induced osteoporosis. *Curr Opin Rheumatol 15*, 454-457. doi:10.1186/ar1372

Cassuto, J., Folestad, A., Gothlin, J. et al. (2018). The key role of proinflammatory cytokines, matrix proteins, RANKL/OPG and Wnt/β-catenin in bone healing of hip arthroplasty patients. *Bone 107*, 66-77. doi:10.1016/j.bone.2017.11.004

Chen, X., Gan, Y., Li, W. et al. (2014). The interaction between mesenchymal stem cells and steroids during inflammation. *Cell Death Dis 5*, e1009. doi:10.1038/cddis.2013.537

Claes, L., Recknagel, S. and Ignatius, A. (2012). Fracture healing under healthy and inflammatory conditions. *Nat Rev Rheumatol 8*, 133-143. doi:10.1038/nrrheum.2012.1

Colnot, C., Thompson, Z., Miclau, T. et al. (2003). Altered fracture repair in the absence of MMP9. *Development 130*, 4123-4133. doi:10.1242/dev.00559

Cramer, T., Yamanishi, Y., Clausen, B. E. et al. (2003). HIF-1α is essential for myeloid cell-mediated inflammation. *Cell 112*, 645-657. doi:10.1016/S0092-8674(03)00154-5

Cui, N., Hu, M. and Khalil, R. A. (2017). Biochemical and biological attributes of matrix metalloproteinases. *Prog Mol Biol Transl Sci 147*, 1-73. doi:10.1016/bs.pmbts.2017.02.005

Curtis, K. M., Gomez, L. A., Rios, C. et al. (2010). EF1α and RPL13a represent normalization genes suitable for RT-qPCR analysis of bone marrow derived mesenchymal stem cells. *BMC Mol Biol 11*, 61. doi:10.1186/1471-2199-11-61

Dengler, V. L., Galbraith, M. and Espinosa, J. M. (2014). Transcriptional regulation by hypoxia inducible factors. *Crit Rev Biochem Mol BIol 49*, 1-15. doi:10.3109/10409238.2013.838205

Denhardt, D. T. and Noda, M. (1998). Osteopontin expression and function: Role in bone remodeling. *J Cell Biochem, Suppl 30-31*, 92-102. doi:10.1002/(SICI)1097-4644(1998)72:30/31+<92::AID-JCB13>3.0.CO;2-A

Dominici, M., Le Blanc, K., Mueller, I. et al. (2006). Minimal criteria for defining multipotent mesenchymal stromal cells. The international society for cellular therapy position statement. *Cytotherapy 8*, 315-317. doi:10.1080/14653240600855905

Donneys, A., Farberg, A. S., Tchanque-Fossuo, C. N. et al. (2012). Deferoxamine enhances the vascular response of bone regeneration in mandibular distraction osteogenesis. *Plast Reconstr Surg 129*, 850-856. doi:10.1097/PRS.0b013e31824422f2

Donneys, A., Ahsan, S., Perosky, J. E. et al. (2013a). Deferoxamine restores callus size, mineralization, and mechanical strength in fracture healing after radiotherapy. *Plast Reconstr Surg 131*, 711e-719e. doi:10.1097/PRS.0b013e3182865c57

Donneys, A., Weiss, D. M., Deshpande, S. S. et al. (2013b). Localized deferoxamine injection augments vascularity and improves bony union in pathologic fracture healing after radiotherapy. *Bone 52*, 318-325. doi:10.1016/j.bone.2012.10.014

Donneys, A., Nelson, N. S., Page, E. E. et al. (2015). Targeting angiogenesis as a therapeutic means to reinforce osteocyte survival and prevent nonunions in the aftermath of radiotherapy. *Head Neck 37*, 1261-1267. doi:10.1002/hed.23744

Donneys, A., Nelson, N. S., Perosky, J. E. et al. (2016). Prevention of radiation-induced bone pathology through combined pharmacologic cytoprotection and angiogenic stimulation. *Bone 84*, 245-252. doi:10.1016/j.bone.2015.12.051

Drager, J., Sheikh, Z., Zhang, Y. L. et al. (2016). Local delivery of iron chelators reduces in vivo remodeling of a calcium phosphate bone graft substitute. *Acta Biomater 42*, 411-419. doi:10.1016/j.actbio.2016.07.037

Drager, J., Ramirez-GarciaLuna, J. L., Kumar, A. et al. (2017). Hypoxia biomimicry to enhance monetite bone defect repair. *Tissue Eng Part A 23*, 1372-1381. doi:10.1089/ten.TEA.2016.0526

El-Jawhari, J. J., Jones, E. and Giannoudis, P. V. (2016). The roles of immune cells in bone healing; what we know, do not know and future perspectives. *Injury 47*, 2399-2406. doi:10.1016/j.injury.2016.10.008

El Khassawna, T., Serra, A., Bucher, C. H. et al. (2017). T lymphocytes influence the mineralization process of bone. *Front Immunol 8*, 562. doi:10.3389/fimmu.2017.00562

Farberg, A. S., Jing, X. L., Monson, L. A. et al. (2012). Deferoxamine reverses radiation induced hypovascularity during bone regeneration and repair in the murine mandible. *Bone 50*, 1184-1187. doi:10.1016/j.bone.2012.01.019

Farberg, A. S., Sarhaddi, D., Donneys, A. et al. (2014). Deferoxamine enhances bone regeneration in mandibular distraction osteogenesis. *Plast Reconstr Surg 133*, 666-671. doi:10.1097/01.prs.0000438050.36881.a9

Foldager, C. B., Munir, S., Ulrik-Vinther, M. et al. (2009). Validation of suitable house keeping genes for hypoxia-cultured human chondrocytes. *BMC Mol Biol 10*, 94. doi:10.1186/1471-2199-10-94

Frenkel, B., White, W. and Tuckermann, J. (2015). Glucocorticoid-induced osteoporosis. *Adv Exp Med Biol 872*, 179-215. doi:10.1007/978-1-4939-2895-8_8

Gaber, T., Dziurla, R., Tripmacher, R. et al. (2005). Hypoxia inducible factor (HIF) in rheumatology: Low O_2! See what HIF can do! *Ann Rheum Dis 64*, 971-980. doi:10.1136/ard.2004.031641

Gaber, T., Schellmann, S., Erekul, K. B. et al. (2011). Macrophage migration inhibitory factor counterregulates dexamethasone-mediated suppression of hypoxia-inducible factor-1 alpha function and differentially influences human CD4+ T cell proliferation under hypoxia. *J Immunol 186*, 764-774. doi:10.4049/jimmunol.0903421

Gaston, M. S. and Simpson, A. H. (2007). Inhibition of fracture healing. *J Bone Joint Surg Br 89*, 1553-1560. doi:10.1302/0301-620x.89b12.19671

Gieseke, F., Schutt, B., Viebahn, S. et al. (2007). Human multipotent mesenchymal stromal cells inhibit proliferation of PBMCs independently of IFNγR1 signaling and IDO expression. *Blood 110*, 2197-2200. doi:10.1182/blood-2007-04-083162

Gomez-Barrena, E., Rosset, P., Lozano, D. et al. (2015). Bone fracture healing: Cell therapy in delayed unions and nonunions. *Bone 70*, 93-101. doi:10.1016/j.bone.2014.07.033

Granero-Molto, F., Weis, J. A., Miga, M. I. et al. (2009). Regenerative effects of transplanted mesenchymal stem cells in fracture healing. *Stem Cells 27*, 1887-1898. doi:10.1002/stem.103

Grogaard, B., Gerdin, B. and Reikeras, O. (1990). The polymorphonuclear leukocyte: Has it a role in fracture healing? *Arch Orthop Trauma Surg 109*, 268-271. doi:10.1007/BF00419942

Gross, T. S., King, K. A., Rabaia, N. A. et al. (2005). Upregulation of osteopontin by osteocytes deprived of mechanical loading or oxygen. *J Bone Miner Res 20*, 250-256. doi:10.1359/jbmr.041004

Grosso, A., Burger, M. G., Lunger, A. et al. (2017). It takes two to tango: Coupling of angiogenesis and osteogenesis for bone regeneration. *Front Bioeng Biotechnol 5*, 68. doi:10.3389/fbioe.2017.00068

Grundnes, O. and Reikeras, O. (1993). The importance of the hematoma for fracture healing in rats. *Acta Orthop Scand 64*, 340-342. doi:10.3109/17453679308993640

Guzey, S., Aykan, A., Ozturk, S. et al. (2016). The effects of desferroxamine on bone and bone graft healing in critical-size bone defects. *Ann Plast Surg 77*, 560-568. doi:10.1097/sap.0000000000000679

Haque, N., Rahman, M. T., Abu Kasim, N. H. et al. (2013). Hypoxic culture conditions as a solution for mesenchymal stem cell based regenerative therapy. *Scientific World Journal 2013*, 632972. doi:10.1155/2013/632972

Hare, J. M., Fishman, J. E., Gerstenblith, G. et al. (2012). Comparison of allogeneic vs autologous bone marrow-derived mesenchymal stem cells delivered by transendocardial injection in patients with ischemic cardiomyopathy: The POSEIDON randomized trial. *JAMA 308*, 2369-2379. doi:10.1001/jama.2012.25321

Henle, P., Zimmermann, G. and Weiss, S. (2005). Matrix metalloproteinases and failed fracture healing. *Bone 37*, 791-798. doi:10.1016/j.bone.2005.06.015

Herman, S., Kronke, G. and Schett, G. (2008). Molecular mechanisms of inflammatory bone damage: Emerging targets for therapy. *Trends Mol Med 14*, 245-253. doi:10.1016/j.molmed.2008.04.001

Hileti, D., Panayiotidis, P. and Hoffbrand, A. V. (1995). Iron chelators induce apoptosis in proliferating cells. *Br J Haematol 89*, 181-187. doi:10.1111/j.1365-2141.1995.tb08927.x

Hoff, P., Gaber, T., Schmidt-Bleek, K. et al. (2011). Immunologically restricted patients exhibit a pronounced inflammation and inadequate response to hypoxia in fracture hematomas. *Immunol Res 51*, 116-122. doi:10.1007/s12026-011-8235-9

Hoff, P., Maschmeyer, P., Gaber, T. et al. (2013). Human immune cells' behavior and survival under bioenergetically restricted conditions in an in vitro fracture hematoma model. *Cell Mol Immunol 10*, 151-158. doi:10.1038/cmi.2012.56

Hoff, P., Gaber, T., Strehl, C. et al. (2016). Immunological characterization of the early human fracture hematoma. *Immunol Res 64*, 1195-1206. doi:10.1007/s12026-016-8868-9

Jowsey, J. (1966). Studies of haversian systems in man and some animals. *J Anat 100*, 857-864. https://wbrg.net/images/stories/references/jowsey_1966_haversian_systems.pdf

Kang, H., Yan, Y., Jia, P. et al. (2016). Desferrioxamine reduces ultrahigh-molecular-weight polyethylene-induced osteolysis by restraining inflammatory osteoclastogenesis via heme oxygenase-1. *Cell Death Dis 7*, e2435. doi:10.1038/cddis.2016.339

Knight, M. N. and Hankenson, K. D. (2013). Mesenchymal stem cells in bone regeneration. *Adv Wound Care (New Rochelle) 2*, 306-316. doi:10.1089/wound.2012.0420

Kolar, P., Schmidt-Bleek, K., Schell, H. et al. (2010). The early fracture hematoma and its potential role in fracture healing. *Tissue Eng Part B Rev 16*, 427-434. doi:10.1089/ten.TEB.2009.0687

Kolar, P., Gaber, T., Perka, C. et al. (2011). Human early fracture hematoma is characterized by inflammation and hypoxia. *Clin Orthop Relat Res 469*, 3118-3126. doi:10.1007/s11999-011-1865-3

Komori, T. (2010). Regulation of osteoblast differentiation by Runx2. *Adv Exp Med Biol 658*, 43-49. doi:10.1007/978-1-4419-1050-9_5

Konnecke, I., Serra, A., El Khassawna, T. et al. (2014). T and B cells participate in bone repair by infiltrating the fracture callus in a two-wave fashion. *Bone 64*, 155-165. doi:10.1016/j.bone.2014.03.052

Kovach, T. K., Dighe, A. S., Lobo, P. I. et al. (2015). Interactions between MSCs and immune cells: Implications for bone healing. *J Immunol Res 2015,* 752510. doi:10.1155/2015/752510

Kovtun, A., Bergdolt, S., Wiegner, R. et al. (2016). The crucial role of neutrophil granulocytes in bone fracture healing. *Eur Cell Mater 32*, 152-162. doi:10.22203/ecm.v032a10

Krzywinska, E. and Stockmann, C. (2018). Hypoxia, metabolism and immune cell function. *Biomedicines 6*, 56. doi:10.3390/biomedicines6020056

Kunkel, E. J. and Butcher, E. C. (2002). Chemokines and the tissue-specific migration of lymphocytes. *Immunity 16*, 1-4. doi:10.1016/S1074-7613(01)00261-8

Kusumbe, A. P., Ramasamy, S. K. and Adams, R. H. (2014). Coupling of angiogenesis and osteogenesis by a specific vessel subtype in bone. *Nature 507*, 323-328. doi:10.1038/nature13145

Le Blanc, K., Tammik, L., Sundberg, B. et al. (2003). Mesenchymal stem cells inhibit and stimulate mixed lymphocyte cultures and mitogenic responses independently of the major histocompatibility complex. *Scand J Immunol 57*, 11-20. doi:10.1046/j.1365-3083.2003.01176.x

Le Blanc, K. and Davies, L. C. (2015). Mesenchymal stromal cells and the innate immune response. *Immunol Lett 168*, 140-146. doi:10.1016/j.imlet.2015.05.004

Lee, J., Byeon, J. S., Lee, K. S. et al. (2016). Chondrogenic potential and anti-senescence effect of hypoxia on canine adipose mesenchymal stem cells. *Vet Res Commun 40*, 1-10. doi:10.1007/s11259-015-9647-0

Lennon, D. P., Edmison, J. M. and Caplan, A. I. (2001). Cultivation of rat marrow-derived mesenchymal stem cells in reduced oxygen tension: Effects on in vitro and in vivo osteochondrogenesis. *J Cell Physiol 187*, 345-355. doi:10.1002/jcp.1081

Li, J., Fan, L., Yu, Z. et al. (2015). The effect of deferoxamine on angiogenesis and bone repair in steroid-induced osteonecrosis of rabbit femoral heads. *Exp Biol Med (Maywood) 240*, 273-280. doi:10.1177/1535370214553906

Li, P., Oparil, S., Feng, W. et al. (2004). Hypoxia-responsive growth factors upregulate periostin and osteopontin expression via distinct signaling pathways in rat pulmonary arterial smooth muscle cells. *J Appl Physiol (1985) 97*, 1550-1558; discussion 1549. doi:10.1152/japplphysiol.01311.2003

Lieu, S., Hansen, E., Dedini, R. et al. (2011). Impaired remodeling phase of fracture repair in the absence of matrix metalloproteinase-2. *Dis Model Mech 4,* 203-211. doi:10.1242/dmm.006304

Liu, W., Shen, S.-M., Zhao, X.-Y. et al. (2012). Targeted genes and interacting proteins of hypoxia inducible factor-1. *Int J Biochem Mol Biol 3*, 165-178. http://www.ijbmb.org/files/IJBMB1203001.pdf

Liu, X., Zhou, C., Li, Y. et al. (2013). SDF-1 promotes endochondral bone repair during fracture healing at the traumatic brain injury condition. *PLoS One 8*, e54077. doi:10.1371/journal.pone.0054077

Liu, X., Tu, Y., Zhang, L. et al. (2014). Prolyl hydroxylase inhibitors protect from the bone loss in ovariectomy rats by increasing bone vascularity. *Cell Biochem Biophys 69*, 141-149. doi:10.1007/s12013-013-9780-8

Liu, Y. Z., Akhter, M. P., Gao, X. et al. (2018). Glucocorticoid-induced delayed fracture healing and impaired bone biomechanical properties in mice. *Clin Interv Aging 13*, 1465-1474. doi:10.2147/CIA.S167431

Luo, Y., He, D. L., Ning, L. et al. (2006). Over-expression of hypoxia-inducible factor-1alpha increases the invasive potency of LNCaP cells in vitro. *BJU Int 98*, 1315-1319. doi:10.1111/j.1464-410X.2006.06480.x

Madrigal, M., Rao, K. S. and Riordan, N. H. (2014). A review of therapeutic effects of mesenchymal stem cell secretions and induction of secretory modification by different culture methods. *J Transl Med 12*, 260. doi:10.1186/s12967-014-0260-8

Martin, D., Galisteo, R. and Gutkind, J. S. (2009). CXCL8/IL8 stimulates vascular endothelial growth factor (VEGF) expression and the autocrine activation of VEGFR2 in endothelial cells by activating NFκB through the CBM (Carma3/Bcl10/Malt1) complex. *J Biol Chem 284*, 6038-6042. doi:10.1074/jbc.C800207200

Matsumoto, T. and Sato, S. (2015). Stimulating angiogenesis mitigates the unloading-induced reduction in osteogenesis in early-stage bone repair in rats. *Physiol Rep 3*, e12335. doi:10.14814/phy2.12335

Mestas, J. and Hughes, C. C. (2004). Of mice and not men: Differences between mouse and human immunology. *J Immunol 172*, 2731-2738. doi:10.4049/jimmunol.172.5.2731

Mizuno, K., Mineo, K., Tachibana, T. et al. (1990). The osteogenetic potential of fracture haematoma. Subperiosteal and intramuscular transplantation of the haematoma. *J Bone Joint Surg Br 72*, 822-829. doi:10.1302/0301-620X.72B5.2211764

Nauta, A. J. and Fibbe, W. E. (2007). Immunomodulatory properties of mesenchymal stromal cells. *Blood 110*, 3499-3506. doi:10.1182/blood-2007-02-069716

O'Toole, E. A., van Koningsveld, R., Chen, M. et al. (2008). Hypoxia induces epidermal keratinocyte matrix metalloproteinase-9 secretion via the protein kinase C pathway. J *Cell Physiol 214*, 47-55. doi:10.1002/jcp.21160

Paiva, K. B. S. and Granjeiro, J. M. (2017). Matrix metalloproteinases in bone resorption, remodeling, and repair. *Prog Mol Biol Transl Sci 148*, 203-303. doi:10.1016/bs.pmbts.2017.05.001

Perlman, R. L. (2016). Mouse models of human disease: An evolutionary perspective. *Evol Med Public Health 2016*, 170-176. doi:10.1093/emph/eow014

Pfeiffenberger, M., Bartsch, J., Hoff, P. et al. (2019). Hypoxia and mesenchymal stromal cells as key drivers of initial fracture healing in an equine in vitro fracture hematoma model. *PLoS One 14*, e0214276. doi:10.1371/journal.pone.0214276

Potian, J. A., Aviv, H., Ponzio, N. M. et al. (2003). Veto-like activity of mesenchymal stem cells: Functional discrimination between cellular responses to alloantigens and recall antigens. *J Immunol 171*, 3426-3434. doi:10.4049/jimmunol.171.7.3426

Qu, Z. H., Zhang, X. L., Tang, T. T. et al. (2008). Promotion of osteogenesis through β-catenin signaling by desferrioxamine. *Biochem Biophys Res Commun 370*, 332-337. doi:10.1016/j.bbrc.2008.03.092

Reinke, S., Geissler, S., Taylor, W. R. et al. (2013). Terminally differentiated CD8+ T cells negatively affect bone regeneration in humans. *Sci Transl Med 5*, 177ra136. doi:10.1126/scitranslmed.3004754

Rozier, P., Maria, A., Goulabchand, R. et al. (2018). Mesenchymal stem cells in systemic sclerosis: Allogenic or autologous approaches for therapeutic use? *Front Immunol 9*, 2938. doi:10.3389/fimmu.2018.02938

Sato, S., Kim, T., Arai, T. et al. (1986). Comparison between the effects of dexamethasone and indomethacin on bone wound healing. *Jpn J Pharmacol 42*, 71-78. doi:10.1254/jjp.42.71

Sawin, P. D., Dickman, C. A., Crawford, N. R. et al. (2001). The effects of dexamethasone on bone fusion in an experimental model of posterolateral lumbar spinal arthrodesis. *J Neurosurg 94*, 76-81. doi:10.3171/spi.2001.94.1.0076

Schallmoser, K. and Strunk, D. (2009). Preparation of pooled human platelet lysate (pHPL) as an efficient supplement for animal serum-free human stem cell cultures. *J Vis Exp,* 1523. doi:10.3791/1523

Schindeler, A., McDonald, M. M., Bokko, P. et al. (2008). Bone remodeling during fracture repair: The cellular picture. *Semin Cell Dev Biol 19*, 459-466. doi:10.1016/j.semcdb.2008.07.004

Schipani, E., Maes, C., Carmeliet, G. et al. (2009). Regulation of osteogenesis-angiogenesis coupling by HIFs and VEGF. *J Bone Miner Res 24*, 1347-1353. doi:10.1359/jbmr.090602

Semenza, G. L. (1998). Hypoxia-inducible factor 1: Master regulator of O_2 homeostasis. *Curr Opin Genet Dev 8*, 588-594. doi:10.1016/S0959-437X(98)80016-6

Seok, J., Warren, H. S., Cuenca, A. G. et al. (2013). Genomic responses in mouse models poorly mimic human inflammatory diseases. *Proc Natl Acad Sci U S A 110*, 3507-3512. doi:10.1073/pnas.1222878110

Shen, X., Wan, C., Ramaswamy, G. et al. (2009). Prolyl hydroxylase inhibitors increase neoangiogenesis and callus formation following femur fracture in mice. *J Orthop Res 27*, 1298-1305. doi:10.1002/jor.20886

Sila-Asna, M., Bunyaratvej, A., Maeda, S. et al. (2007). Osteoblast differentiation and bone formation gene expression in strontium-inducing bone marrow mesenchymal stem cell. *Kobe J Med Sci 53*, 25-35. http://www.med.kobe-u.ac.jp/journal/contents/53/25.pdf

Soehnlein, O., Lindbom, L. and Weber, C. (2009). Mechanisms underlying neutrophil-mediated monocyte recruitment. *Blood 114*, 4613-4623. doi:10.1182/blood-2009-06-221630

Stamenkovic, I. (2003). Extracellular matrix remodelling: The role of matrix metalloproteinases. *J Pathol 200*, 448-464. doi:10.1002/path.1400

Stewart, R., Goldstein, J., Eberhardt, A. et al. (2011). Increasing vascularity to improve healing of a segmental defect of the rat femur. *J Orthop Trauma 25*, 472-476. doi:10.1097/BOT.0b013e31822588d8

Strehl, C., Ehlers, L., Gaber, T. et al. (2019). Glucocorticoids-all-rounders tackling the versatile players of the immune system. *Front Immunol 10*, 1744. doi:10.3389/fimmu.2019.01744

Tachibana, T., Matsubara, T., Mizuno, K. et al. (1991). Enhance-

ment of new bone formation by hematoma at fracture site. *Nihon Seikeigeka Gakkai Zasshi 65*, 349-358.

Takao, K. and Miyakawa, T. (2015). Genomic responses in mouse models greatly mimic human inflammatory diseases. *Proc Natl Acad Sci U S A 112*, 1167-1172. doi:10.1073/pnas.1401965111

Thomas, M. V. and Puleo, D. A. (2011). Infection, inflammation, and bone regeneration: A paradoxical relationship. *J Dent Res 90*, 1052-1061. doi:10.1177/0022034510393967

Toben, D., Schroeder, I., El Khassawna, T. et al. (2011). Fracture healing is accelerated in the absence of the adaptive immune system. *J Bone Miner Res 26*, 113-124. doi:10.1002/jbmr.185

Varghese, S. (2006). Matrix metalloproteinases and their inhibitors in bone: An overview of regulation and functions. *Front Biosci 11*, 2949-2966. doi:10.2741/2024

Vimalraj, S., Arumugam, B., Miranda, P. J. et al. (2015). Runx2: Structure, function, and phosphorylation in osteoblast differentiation. *Int J Biol Macromol 78*, 202-208. doi:10.1016/j.ijbiomac.2015.04.008

Wagegg, M., Gaber, T., Lohanatha, F. L. et al. (2012). Hypoxia promotes osteogenesis but suppresses adipogenesis of human mesenchymal stromal cells in a hypoxia-inducible factor-1 dependent manner. *PLoS One 7*, e46483. doi:10.1371/journal.pone.0046483

Wan, C., Gilbert, S. R., Wang, Y. et al. (2008). Role of hypoxia inducible factor-1 alpha pathway in bone regeneration. *J Musculoskelet Neuronal Interact 8*, 323-324. http://www.ismni.org/jmni/pdf/34/18WAN.pdf

Wang, G., Shen, G. and Yin, T. (2017a). In vitro assessment of deferoxamine on mesenchymal stromal cells from tumor and bone marrow. *Environ Toxicol Pharmacol 49*, 58-64. doi:10.1016/j.etap.2016.11.014

Wang, L., Jia, P., Shan, Y. et al. (2017b). Synergistic protection of bone vasculature and bone mass by desferrioxamine in osteoporotic mice. *Mol Med Rep 16*, 6642-6649. doi:10.3892/mmr.2017.7451

Waters, R. V., Gamradt, S. C., Asnis, P. et al. (2000). Systemic corticosteroids inhibit bone healing in a rabbit ulnar osteotomy model. *Acta Orthop Scand 71*, 316-321. doi:10.1080/000164700317411951

Wu, Y., Lucia, K., Lange, M. et al. (2014). Hypoxia inducible factor-1 is involved in growth factor, glucocorticoid and hypoxia mediated regulation of vascular endothelial growth factor-A in human meningiomas. *J Neurooncol 119*, 263-273. doi:10.1007/s11060-014-1503-5

Xing, K., Gu, B., Zhang, P. et al. (2015). Dexamethasone enhances programmed cell death 1 (PD-1) expression during T cell activation: An insight into the optimum application of glucocorticoids in anti-cancer therapy. *BMC Immunol 16*, 39. doi:10.1186/s12865-015-0103-2

Yao, Q., Liu, Y., Tao, J. et al. (2016). Hypoxia-mimicking nanofibrous scaffolds promote endogenous bone regeneration. *ACS Appl Mater Interfaces 8*, 32450-32459. doi:10.1021/acsami.6b10538

Yellowley, C. (2013). CXCL12/CXCR4 signaling and other recruitment and homing pathways in fracture repair. *Bonekey Rep 2*, 300. doi:10.1038/bonekey.2013.34

Zeng, H. L., Zhong, Q., Qin, Y. L. et al. (2011). Hypoxia-mimetic agents inhibit proliferation and alter the morphology of human umbilical cord-derived mesenchymal stem cells. *BMC Cell Biol 12*, 32. doi:10.1186/1471-2121-12-32

Zhang, J., Huang, X., Wang, H. et al. (2015). The challenges and promises of allogeneic mesenchymal stem cells for use as a cell-based therapy. *Stem Cell Res Ther 6,* 234. doi:10.1186/s13287-015-0240-9

Zhang, W., Li, G., Deng, R. et al. (2012). New bone formation in a true bone ceramic scaffold loaded with desferrioxamine in the treatment of segmental bone defect: A preliminary study. *J Orthop Sci 17*, 289-298. doi:10.1007/s00776-012-0206-z

Competing financial interest statement

The authors declare that they have no conflict of interest.

Authors' contributions

Study design: MP, AL, TG; Data collection and analysis: MP, AL, TG; Drafting manuscript: MP, AL, TG; Data discussion and interpretation: MP, PH, CTR, FB, AL, TG; Revising manuscript: MP, PH, CTR, FB, AL, TG.

Acknowledgements

The authors would like to thank Manuela Jakstadt for excellent technical assistance. FACS analyses were performed together with the Core Facility at the German Rheumatism Research Centre. Bone marrow was provided from the "Tissue Harvesting" core facility of the BCRT.

The study was funded by the German Federal Ministry for Education and Research (project no. 031A334). The work of Timo Gaber was funded by the Deutsche Forschungsgemeinschaft (project no. 353142848). We acknowledge support from the German Research Foundation (DFG) and the Open Access Publication Fund of Charité – Universitätsmedizin Berlin. Funding bodies did not have any role in designing the study, in collecting, analyzing and interpreting the data, in writing this manuscript, and in deciding to submit it for publication.